

Gaseous detectors - 2

Silvia Masciocchi,
GSI and University of Heidelberg

*SS2017, Heidelberg
May 17, 2017*

Ionization mode:

Full charge collection

No multiplication – gain = 1

Proportional mode:

Multiplication of ionization

Signal proportional to ionization

Measurement of dE/dx

Secondary avalanches need quenching

Gain $\sim 10^4 - 10^5$

Limited proportional mode (saturated, streamer):

Strong photoemission

Strong quenches or pulsed HV

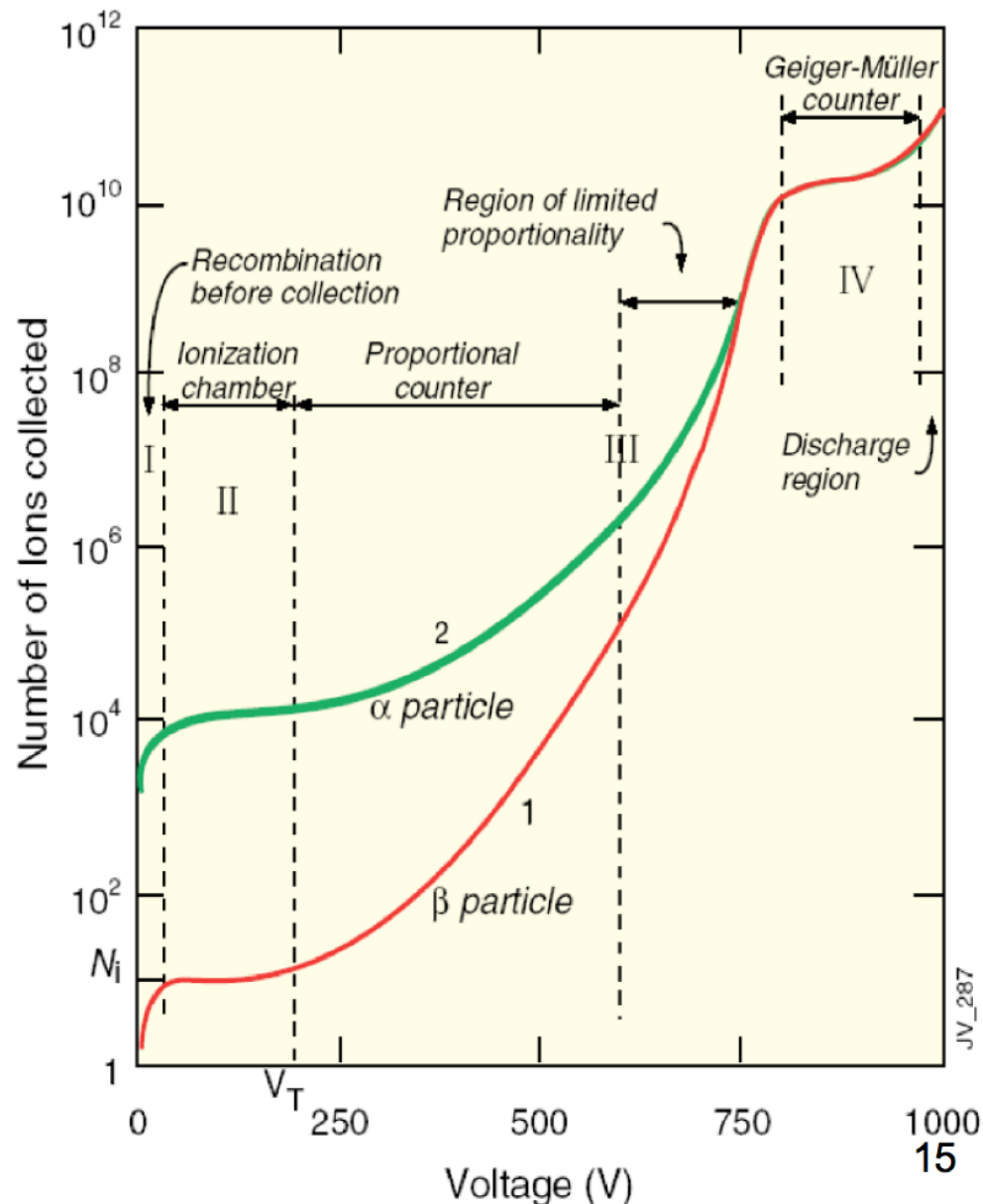
Gain $\sim 10^{10}$

Geiger mode:

Massive photoemission

Full length of anode wire affected

Discharge stopped by HV cut



Gas detectors: outline

- Ionization in gas
- Charge transport in gas: electron and ion mobility
- Diffusion
- Drift velocity
- Charge multiplication / gas amplification

- Ionization chamber
- Proportional counter
 - Multiwire proportional chambers

- Drift chambers
 - Cylindrical wire chambers
 - Jet drift chambers
- Time projection chambers

**Last lecture,
May 10**

Gas detectors: today

- Ionization in gas
- Charge transport in gas: electron and ion mobility
- Diffusion
- Drift velocity
- Charge multiplication / gas amplification

- Ionization chamber
- Proportional counter
 - Multiwire proportional chambers

- Drift chambers
 - Cylindrical wire chambers
 - Jet drift chambers
- Time projection chambers

- MWPC spatial resolution: wire stability and limitation in spatial resolution
- → micro-pattern gas detectors (microstrip gas detector, gas electron multiplier)

**Last lecture,
May 10**

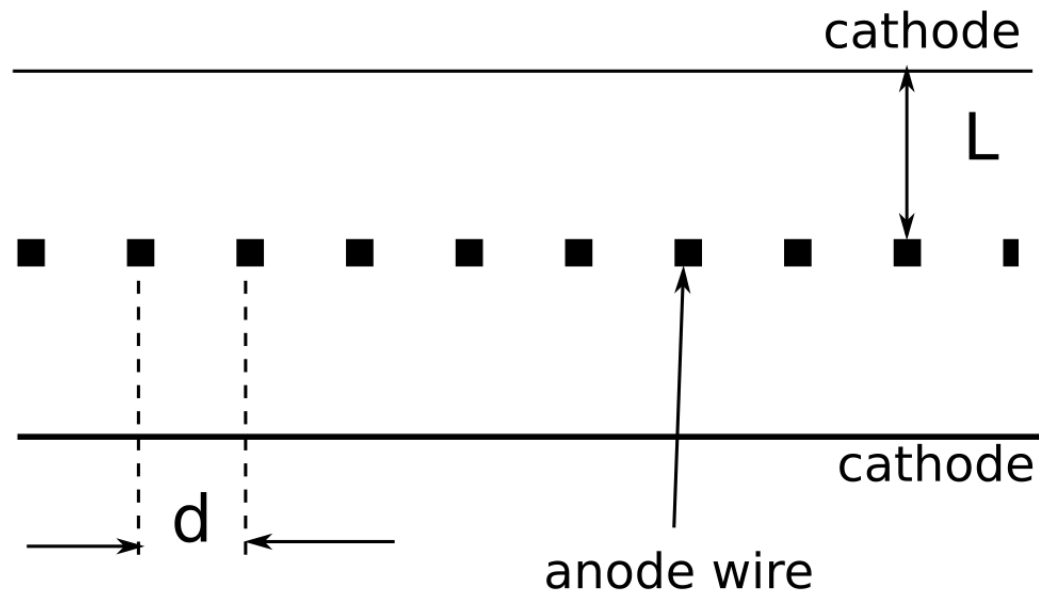
Multi-wire proportional chamber - MWPC

Planar arrangement of proportional counters, without separating walls

G. Charpak et al., NIM 62 (1968) 202

Nobel prize 1992

REMINDER



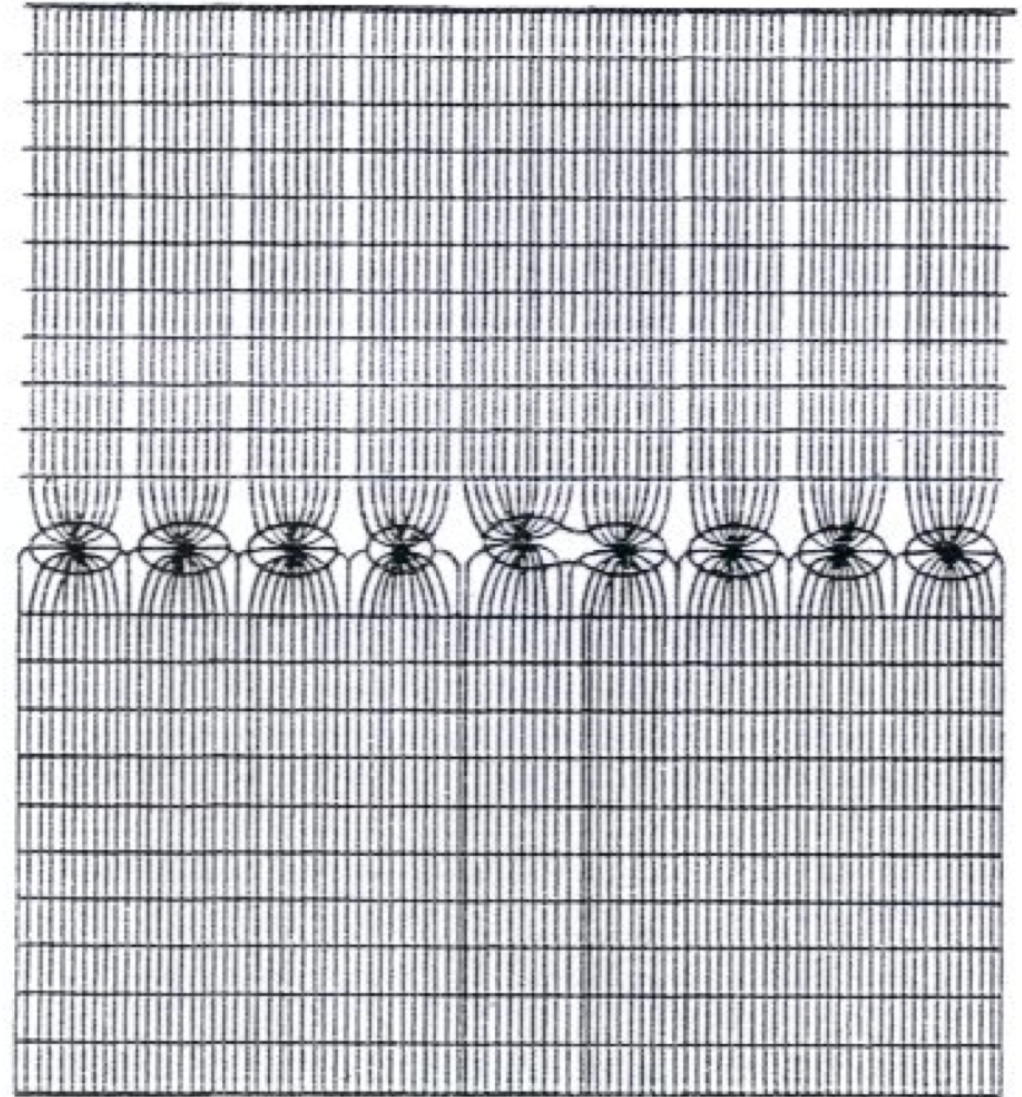
Tracking of charged particles, large area coverage, high rate capability, moderate pid capabilities via dE/dx

Field lines, and equipotential lines

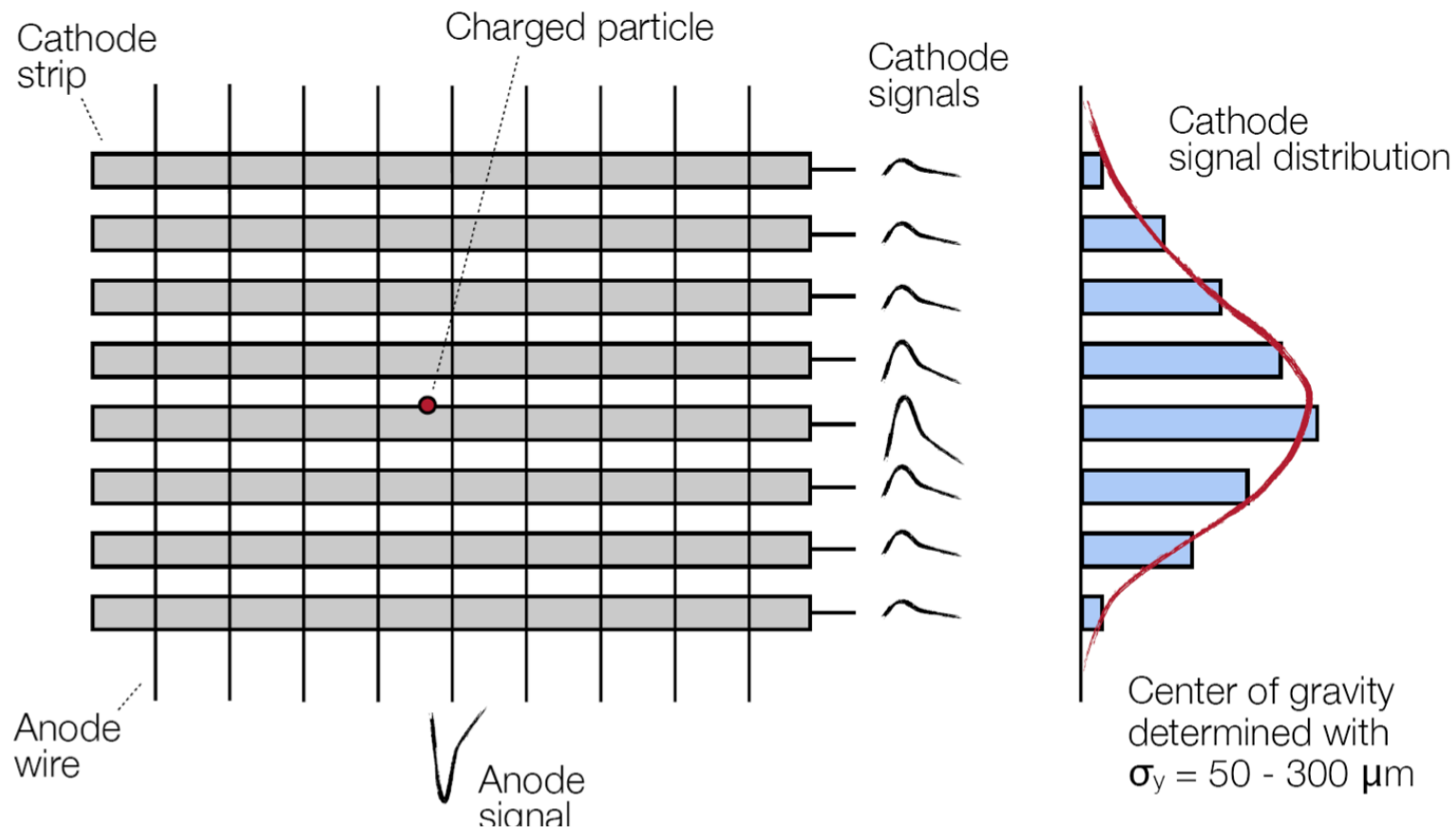
Difficulty evident:

Even small geometric displacements of an individual wire lead to effects on the field quality

Need of high mechanical precision, both for geometry and wire tension (electrostatic effects and gravitational wire sag, see later)



- Perpendicular to wire: since information comes only from closest wire $\rightarrow \delta x = d/\sqrt{12} = \text{e.g. } 577 \mu\text{m}$ for $d = 2 \text{ mm}$ not quite so precise!
- Then: segment the cathode in strips: the induced signal is spread over more strips. Using the **center of gravity** of the signal (charge sharing), high precision of $50 - 300 \mu\text{m}$ can be reached



When 2 particles cross the MWPC, with only one orientation of the cathode strips we are left with the ambiguity of the combinations of signals ●● ○○
→ 4 possibilities: 2 real, 2 ghosts

Possible solution: use **different orientation of strips on the second cathode plane**

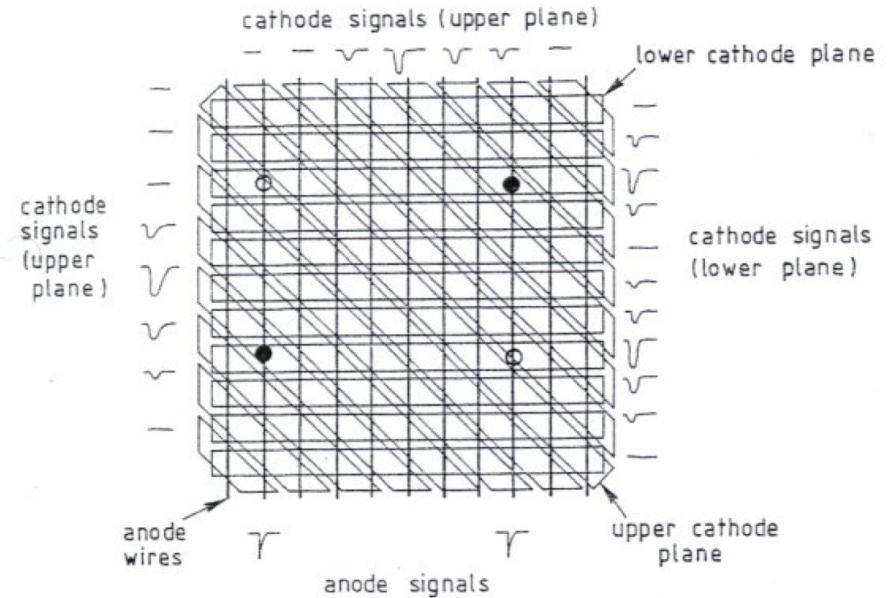
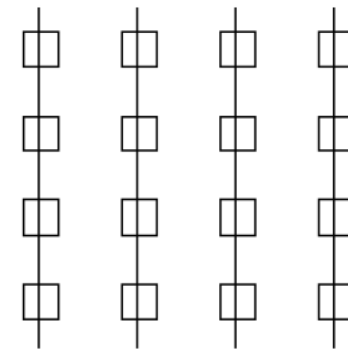


Illustration of the resolution of ambiguities for two particles registered in a multi-wire proportional chamber

For high multiplicities and high hit density: segment the **cathode in pads** for a 2-dimensional measurement

Disadvantage: number of readout channels grows quadratically (**expensive!**)



MWPC – stability of wire geometry

Can the resolution be improved by mounting the wires closer to each other?

Practical difficulty in stretching wires precisely, closer than 1 mm:

- Electrostatic repulsion between anode wires (particularly for long wires)
→ can lead to “staggering”

To void this, the wire tension T has to be larger than a critical value T_0 (order of 0.5 N for wires of 1 m and typical chamber geometry)

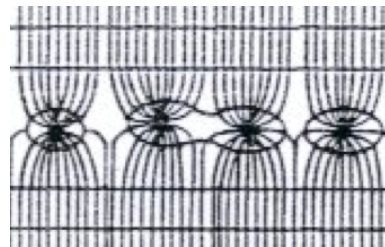
- For horizontal wires problem of gravity → sag



$$f = \frac{\pi r_i^2}{8} \rho g \frac{l^2}{T} = \frac{m l g}{8 T}$$

gold-plated W-wire $r_i = 15 \mu\text{m}$, T as above → $f = 34 \mu\text{m}$ → visible difference in gain

And remember:



MWPC → straw tube chambers

Some of these troubles are addressed by straw tube chambers: compact assembly of **single-wire proportional chambers** (see last week, LHCb outer tracker example)

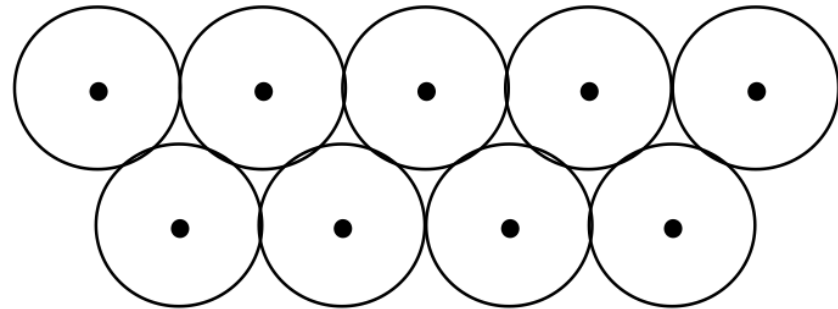
Cylindrical wall = cathode

Aluminized mylar foil

Introduced in the 1990s

Straw diameter: 5-10 mm

Can be operated at overpressure



- Further very big advantage: a broken wire affects only one cell!! In a MWPC: large area, if not the entire chamber
- Spatial resolution: down to 160 μm
- Short drift lengths → high rates possible!
 - operation in magnetic field possible without degradation of resolution!

MWPC – wire aging

Avalanche formation can be considered as a micro plasma discharge.

Consequences:

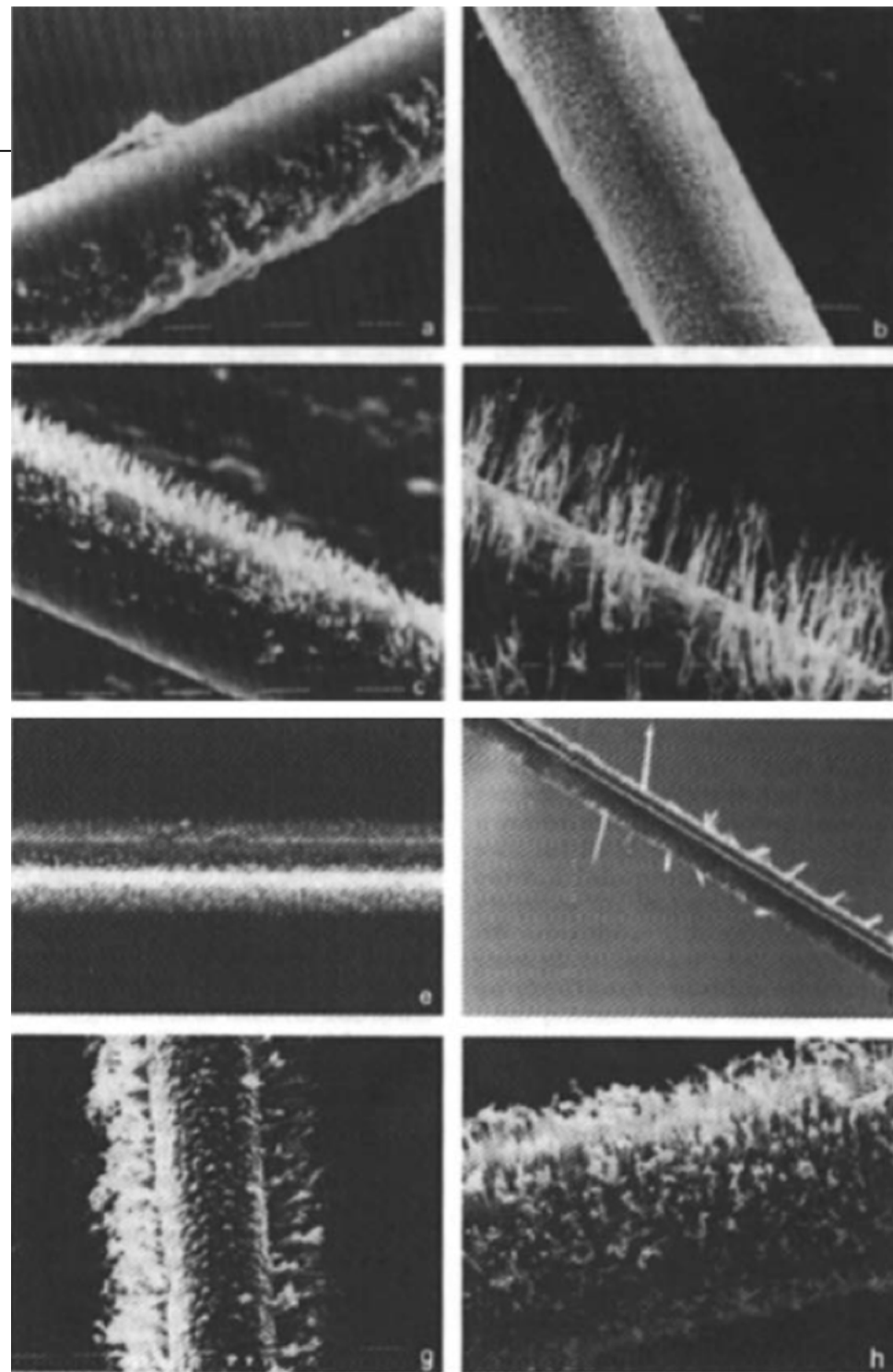
- Formation of radicals, i.e. molecule fragments
- Polymerization yields long chains of molecules
- Polymers may be attached to the electrodes
- Reduction of gas amplification

Important: AVOID unnecessary contaminations!

Harmful are:

- Halogens or halogen compounds
- Silicon compounds
- Carbonates, halocarbons
- Polymers
- Oil, fat ...

Can wires be avoided?

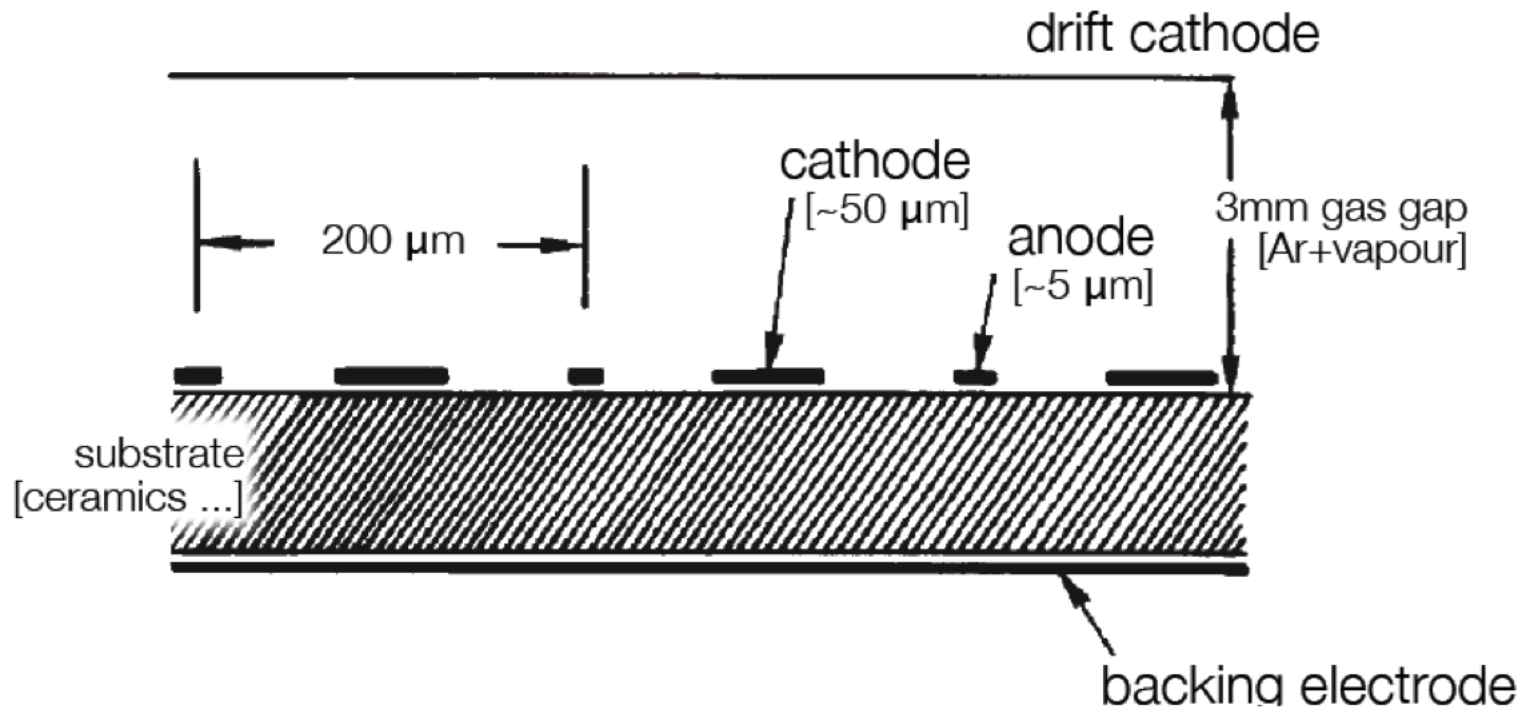


Micro-strip gas chambers

Anodes can be realized via microstructures on dielectrics:

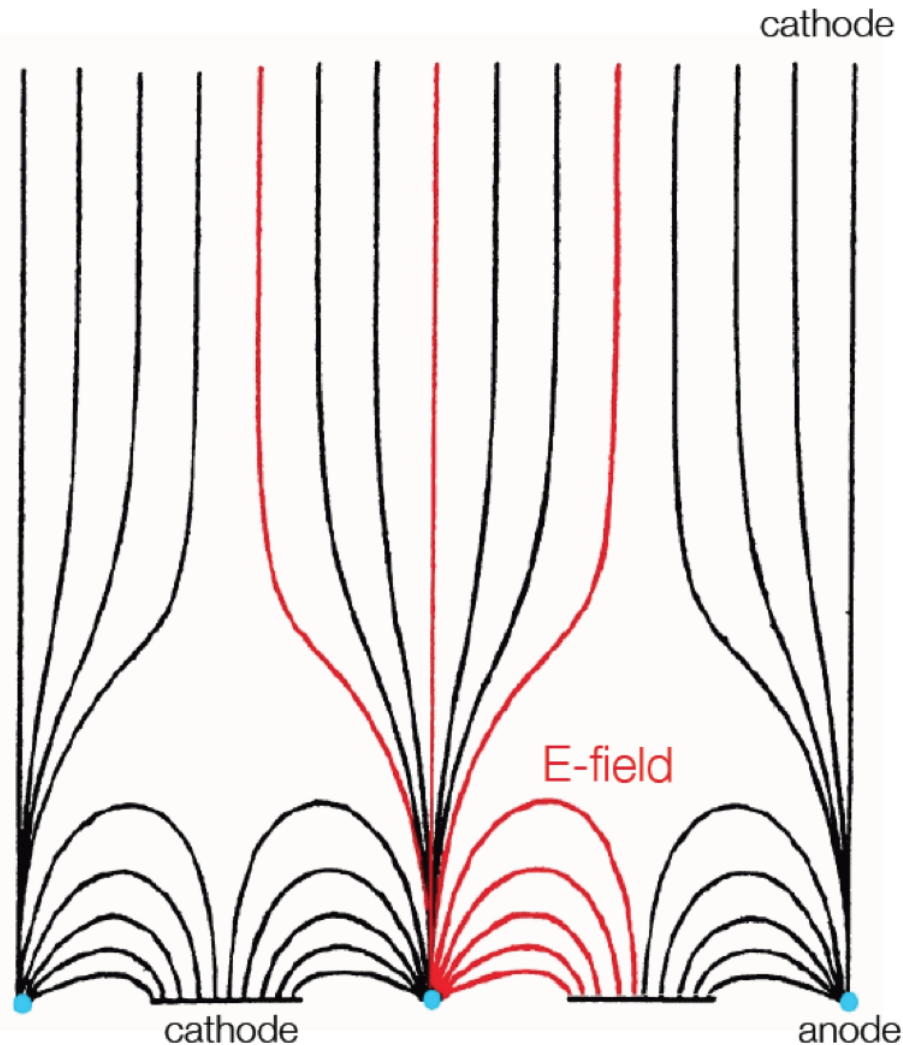
- Simple construction (today)
- Enhanced stability and flexibility
- Improved rate capabilities

First MSGS realized in the 1990s



Micro-strip gas chambers

Schematics of MSGC field lines



Advantages:

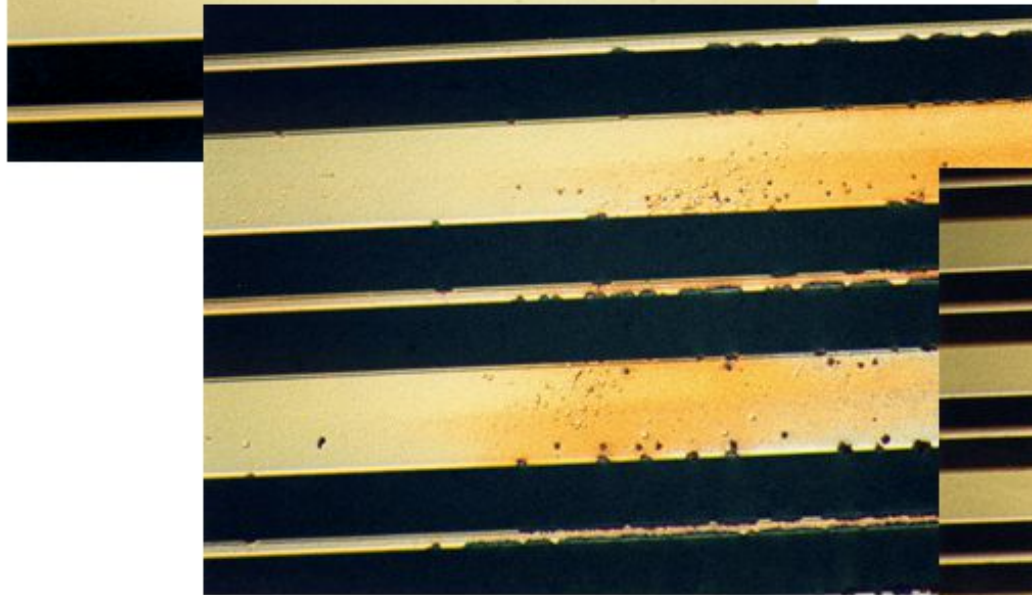
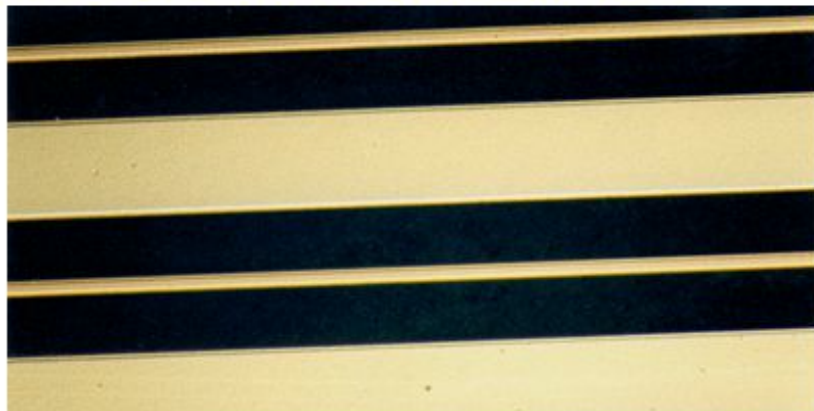
- High field directly above anode
- Ions drift only 100 μm \rightarrow low dead time, high rate capability without build-up of space charge
- Resolution: fine structures can be fabricated by electron lithography on ceramics, glass or plastic foils on which a metal film was previously evaporated

Problems:

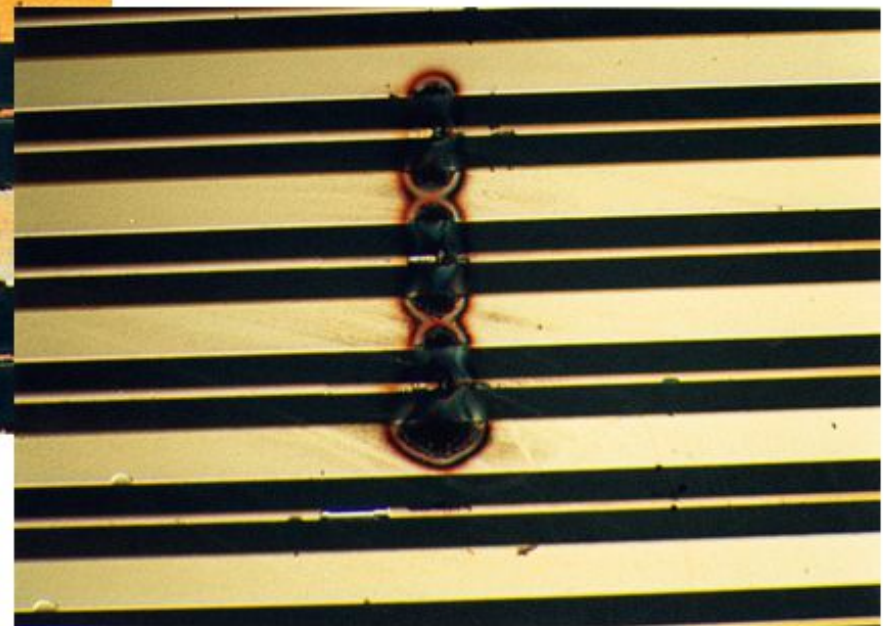
- Charging of insulating structures
- Time dependent gain, sparks, anode destruction, corrosion of insulator
- Lifetime of detector too limited

Not quite a success!

MSGC DISCHARGE PROBLEMS:



MICRODISCHARGES

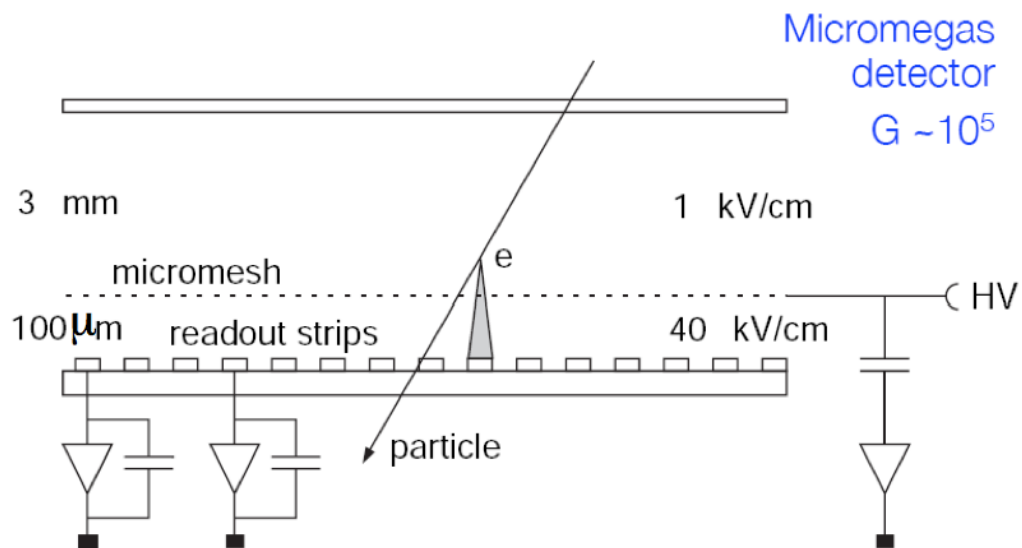


FULL BREAKDOWN

Micro-strip gas chambers

Mitigation of problems: add an intermediate structure

1. Micromegas: fine cathode mesh collects ions. Still fast. No wires

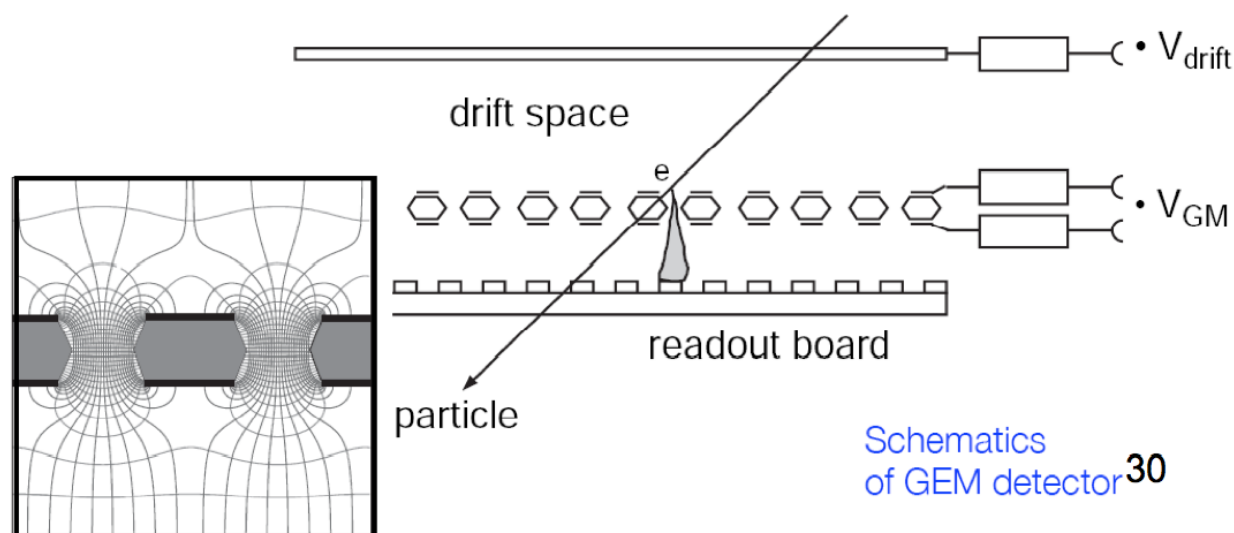


2. Gas Electron Multiplier (GEM)

F. Sauli, CERN, ~1997

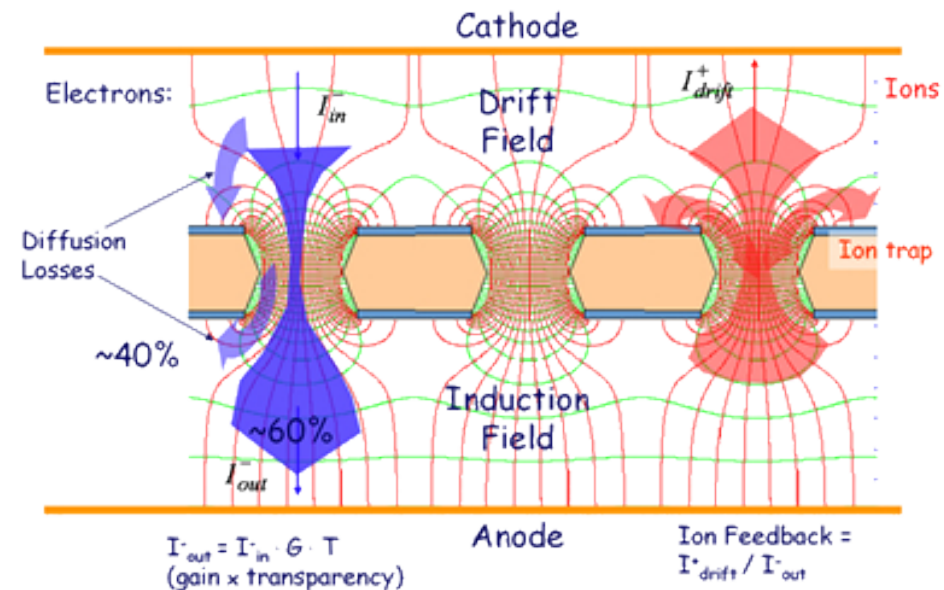
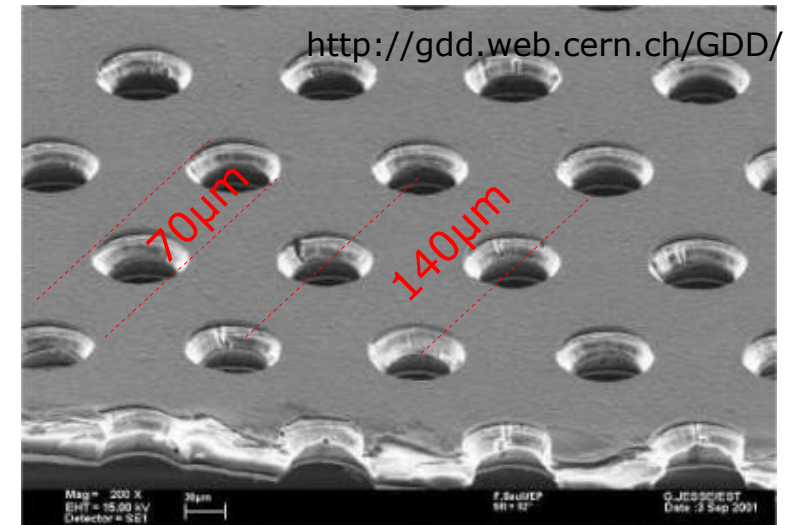
Offers a pre-amplification and allows reduced electric field in the vicinity of the node structures.

Ease of construction again partly eliminated, risk of discharge on foil (huge capacitance)



GEM detectors

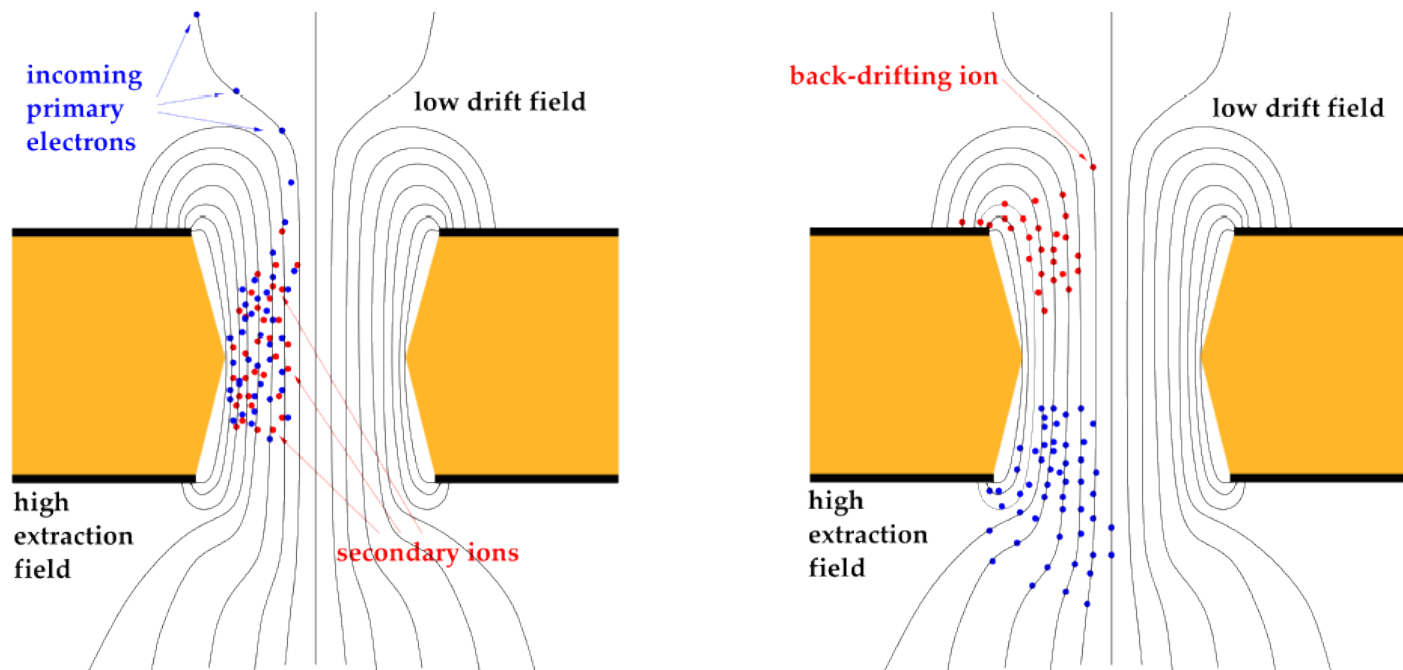
- Copper coated Kapton foils ($50\mu\text{m}$)
 - Holes etched into the foil
 - Size $\sim 70\mu\text{m}$
 - Distance $\sim 140\mu\text{m}$
-
- Apply voltage on copper coating
 - Up to $\Delta U \approx 500\text{V}$
 - Fields up to $\sim 100\text{kV/cm}$
 - Holes act as multiplication channels
 - Natural Ion Back-Flow (IBF) suppression



<http://www.infn.it/csn5/joomla/GEMINI/>

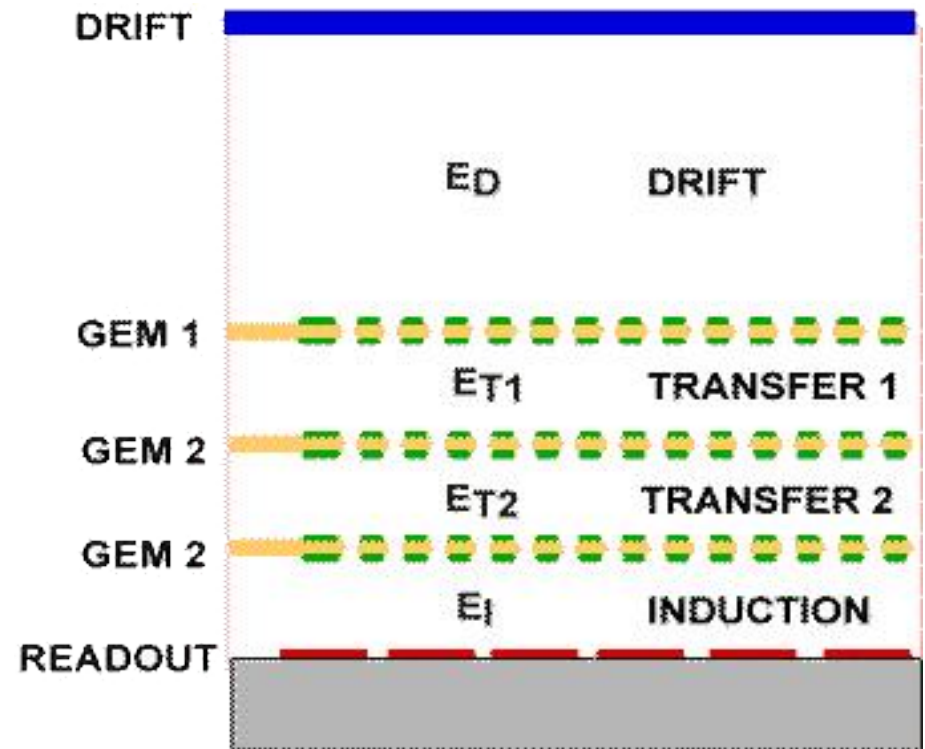
GEM detectors - Ion Back-Flow

- Natural IBF suppression:
 - Asymmetric mobility [low for ions – high for electrons]
 - Electrons move to larger fields in the amplification channel
 - More ions are produced at the edges → trajectory ends on top electrode
 - Asymmetric field [drift – induction]
 - Many field lines end on top electrons (ion capture)
 - Transfer region allows for good electron extraction



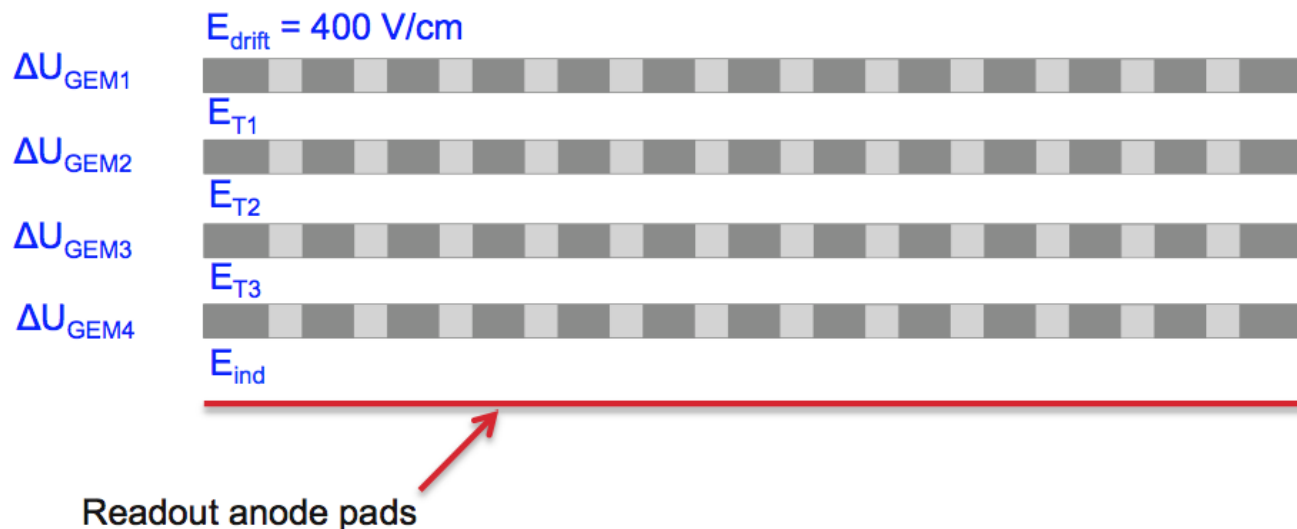
GEM detectors - Setting up GEM stacks

- Usually more than 1 GEM foil used (often 3, or 4)
- Many advantages
 - Larger gain at lower ΔU \rightarrow higher stability
 - Allows for higher total gain (cascaded amplification)
 - Large parameter space \rightarrow tuning of voltages to obtain low IBF



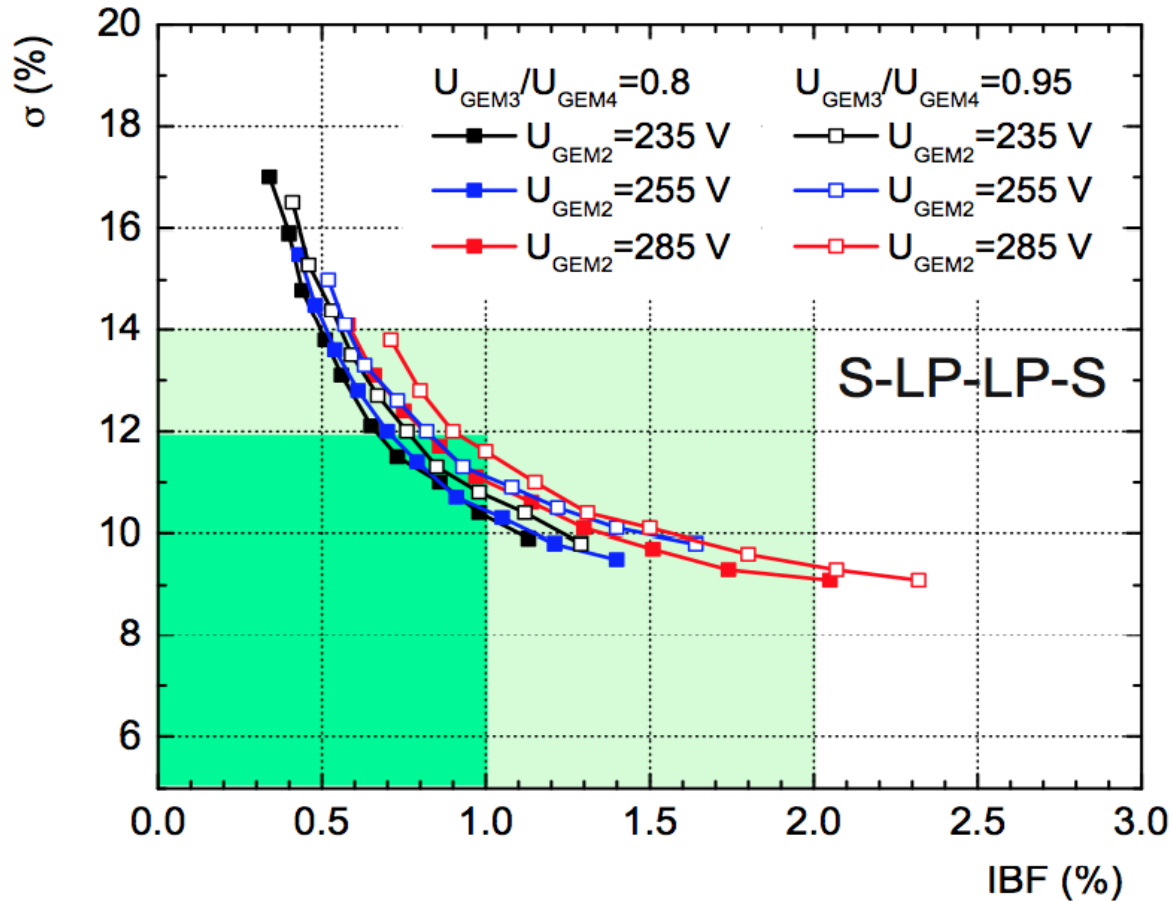
4-GEM SYSTEMS

- Solution is a 4-GEM system
- Optimization with respect to Ion Backflow and energy resolution requires careful multi-parameter scan



- Requirements: IBF < 1(2)% and $\sigma(^{55}\text{Fe}) < 12(14)\%$ at Gain=2000 and $E_{\text{drift}}=400 \text{ V/cm}$ in Ne-CO₂-N₂(90-10-5), stable operation
- Optimization parameters:
 - Field and voltage settings: E_{T1} , E_{T2} , E_{T3} , E_{IND} , ΔU_{GEM1} , ΔU_{GEM2} , ΔU_{GEM3} , ΔU_{GEM4}
 - GEM hole pitch: small (90 μm), standard (140 μm), medium (200 μm), large (280 μm)

TDR BASELINE SOLUTION



TPC Upgrade TDR
CERN-LHCC 2013-020

- Working point that fulfills TDR requirements was identified with 4-GEM system and foils of different hole pitch
- TDR requirements were demonstrated to be conservative

GEMs for the ALICE TPC upgrade

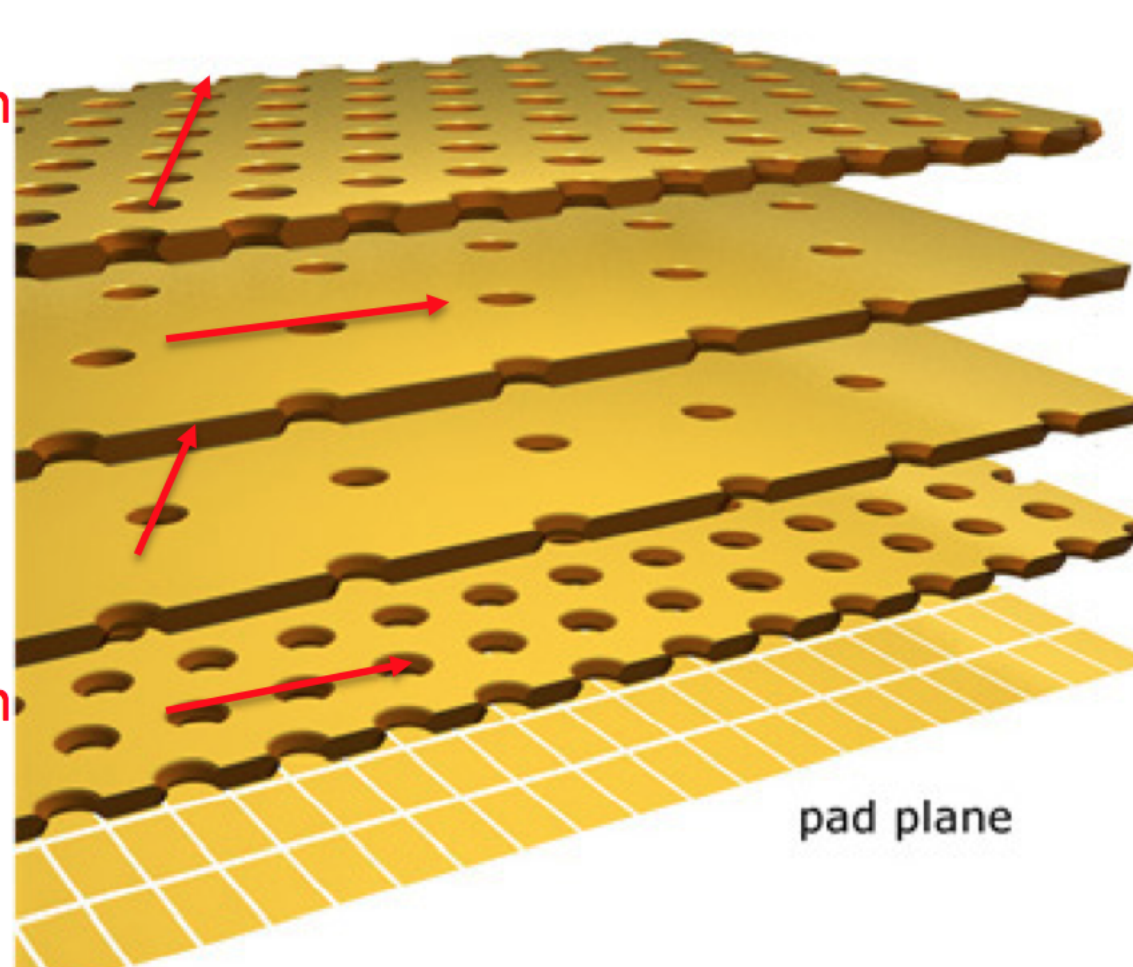
Hole pitch and orientation count:

Standard Pitch
not rotated

Large Pitch
rotated

Large Pitch
not rotated

Standard Pitch
rotated



Drift chambers

Obtain spatial information from the electron drift time t_D

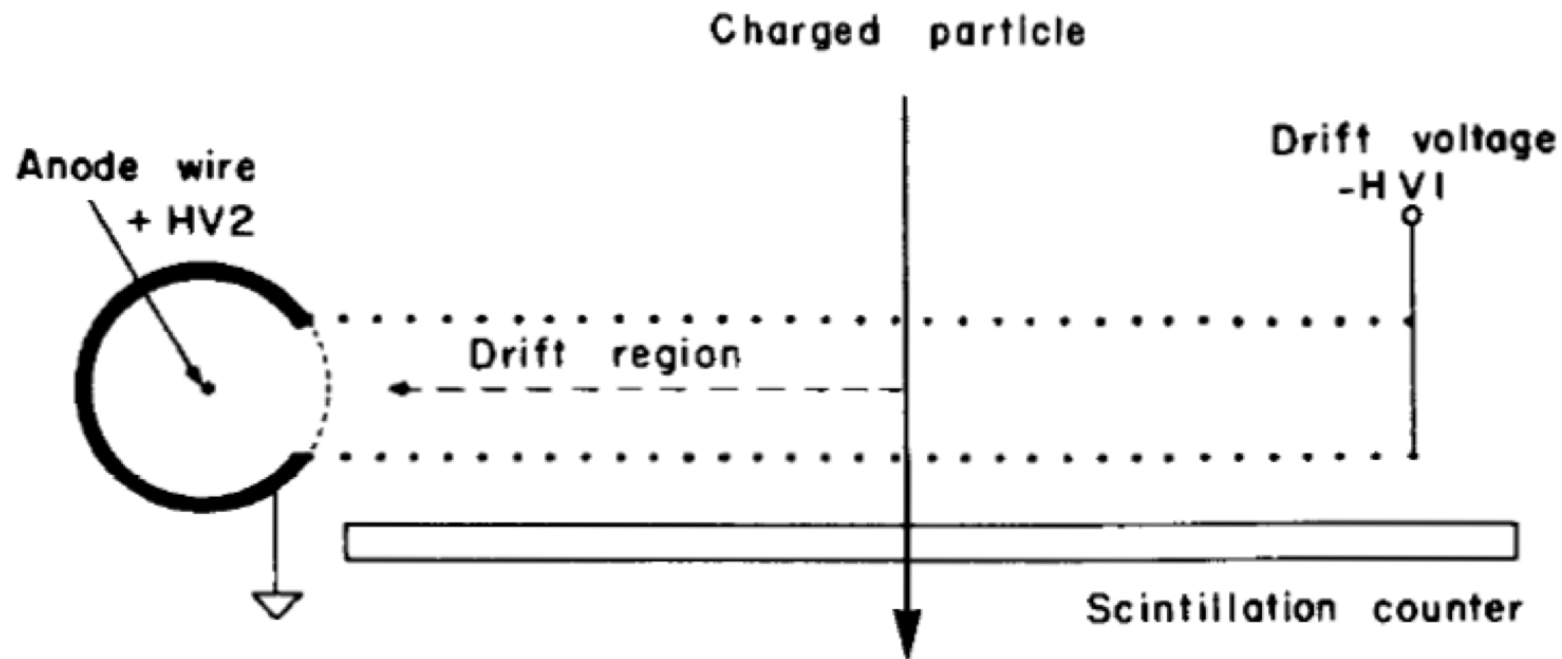
Need to know t_0 , from a fast scintillator or beam timing

If v_D^- electron drift velocity:

Or, if the drift velocity changes along the electron path:

$$x = v_D^- \cdot \Delta t$$

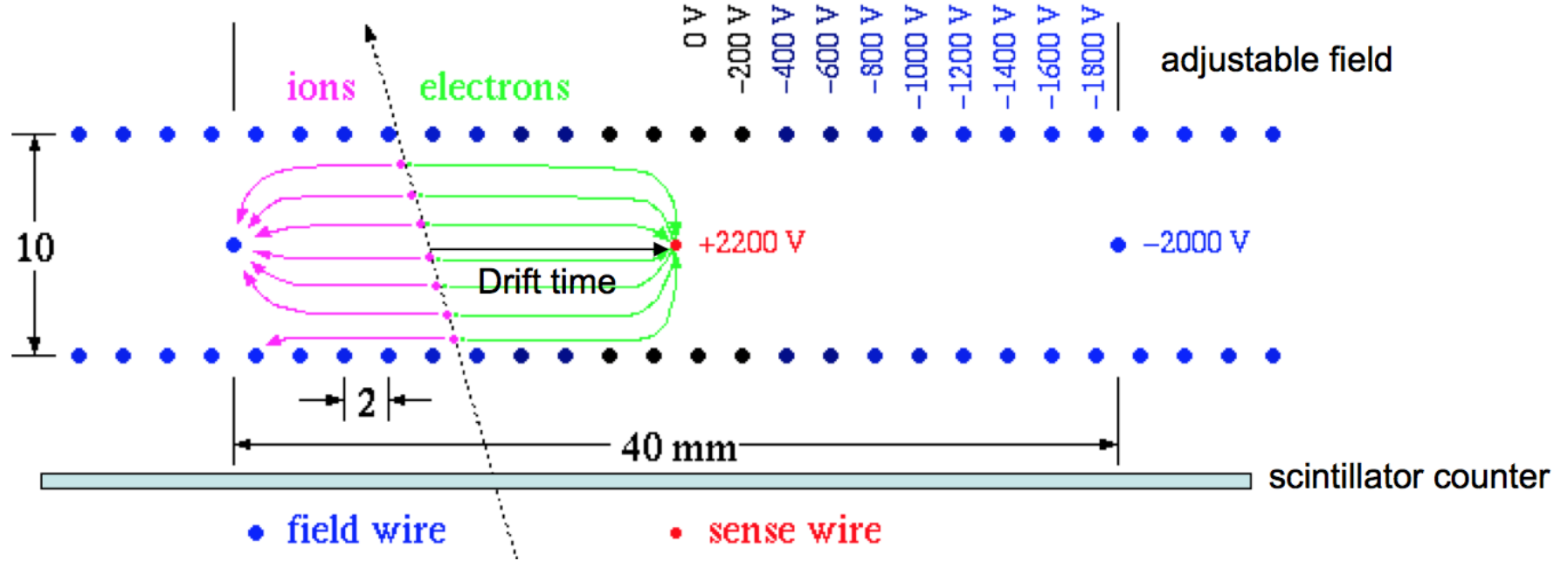
$$x = \int_{t_0}^{t_D} v_D^- (t) dt$$



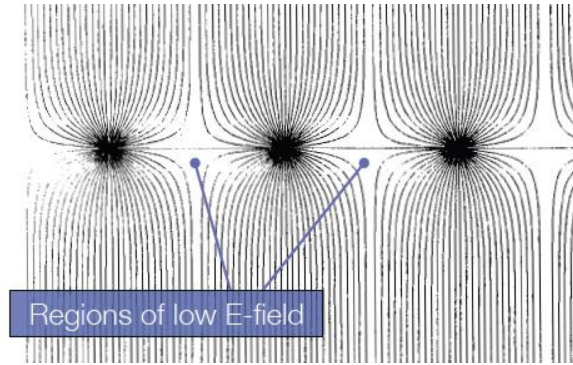
Invented by A. Walenta, J. Heintze in 1970 at Phys. Inst. U.Heidelberg NIM 92 (1971) 373

Drift chambers

Needs well defined drift field → introduce additional field wires in between anode wires



Drift chambers: field wires

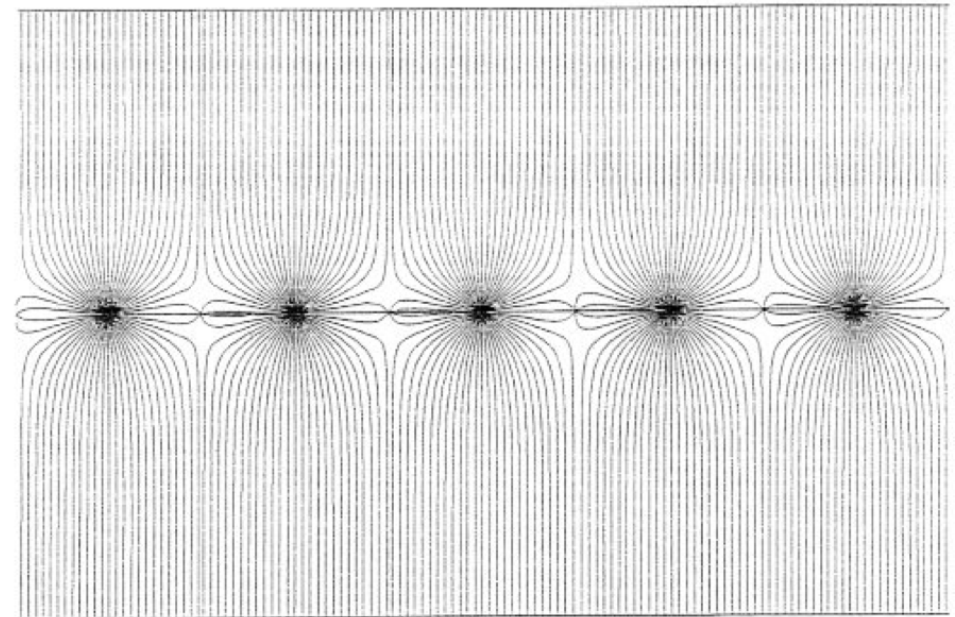
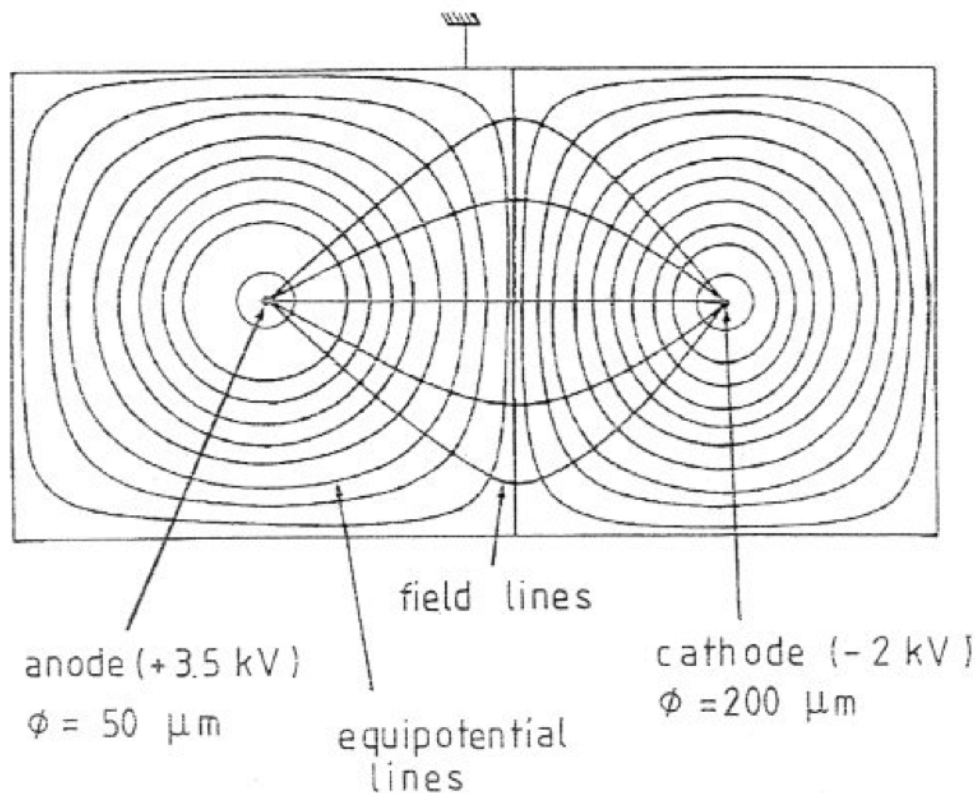


MWPC:

regions of very low electric field between anode wires

Here add **field wires** at negative potential wrt anode wires → strongly improves the quality of the field!

This is essential for drift chambers where **spatial resolution** is dominated by **drift time variations** (and not by segmented electrode structure)

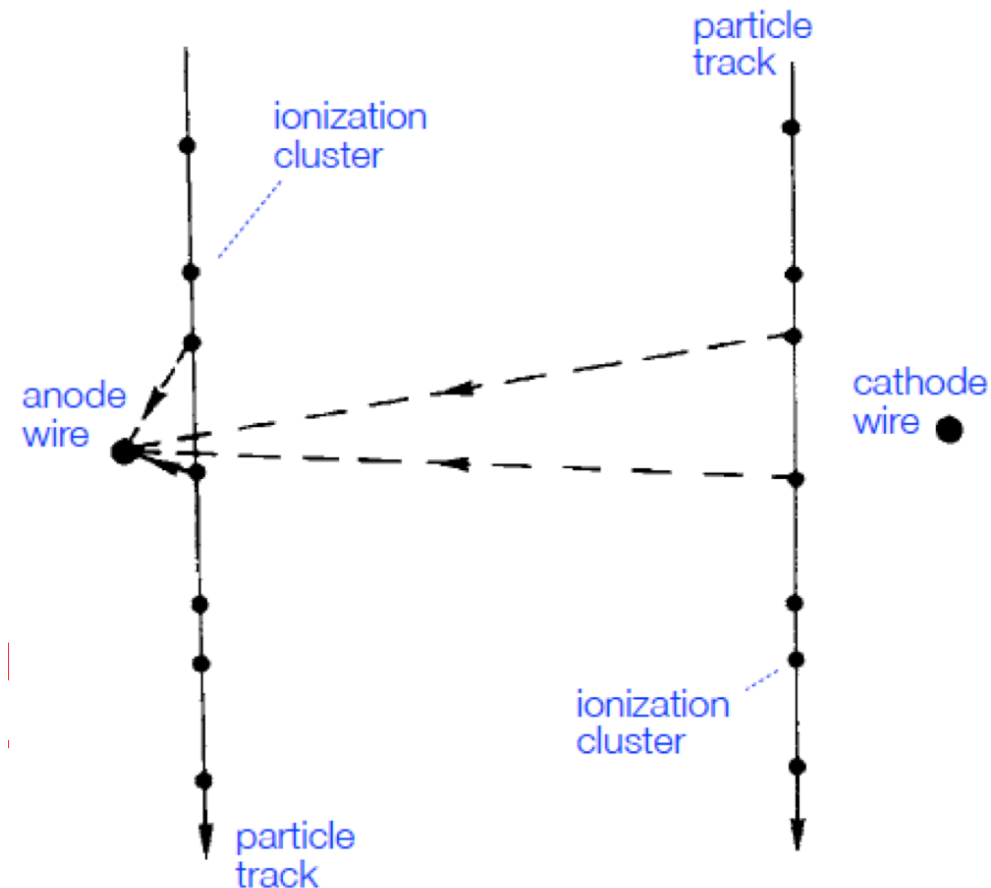


Drift chambers: spatial resolution

Resolution is determined by the accuracy of drift time measurement

Influenced by:

- Diffusion: $\sigma_{\text{diff}} \sim \sqrt{x}$
- δ -electrons: σ_{δ} is independent of drift length \rightarrow constant term in resolution
- Electronics: $\sigma_{\text{electronics}} = \text{constant}$, also independent of drift length
- Primary ionization statistics: $\sigma_{\text{prim}} \sim 1/x$
Spatial fluctuations of charge-carrier production result in large drift-path differences for particle trajectories close to the anode. It has minor influence for tracks far away from the anode



Drift chambers: spatial resolution

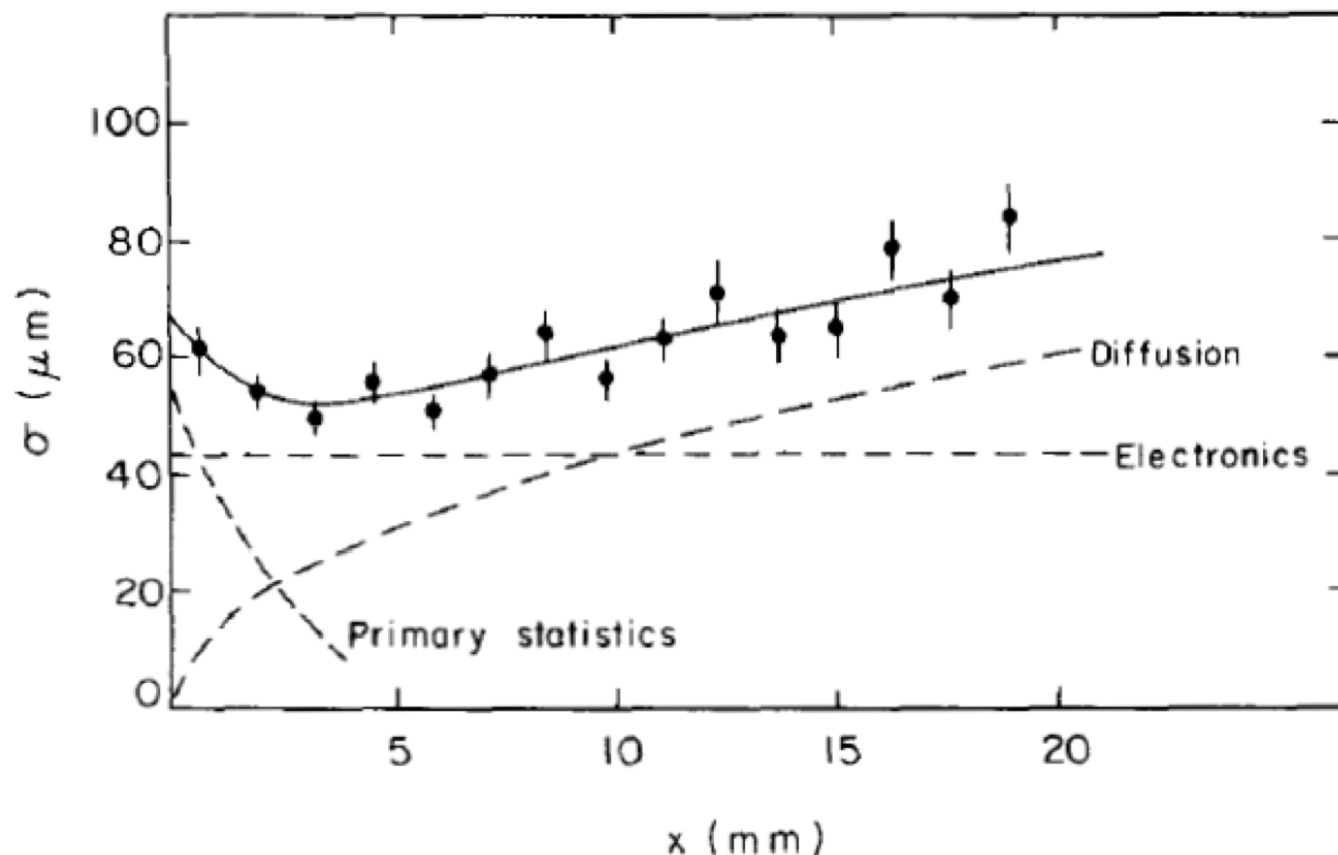
$$\sigma_x^2 = \underbrace{\left(\frac{1}{64N^2}\right) \cdot \frac{1}{x^2}}_{1^{\text{st}} \text{ ionization statistics}} + \underbrace{\frac{2D}{v_d} \cdot x}_{\text{diffusion}} + \underbrace{\sigma_{\text{const}}^2}_{\text{electronics } \delta\text{-electrons}}$$

Possible improvements:

- Increase N by increasing the pressure
- Decrease D by increasing the pressure

$$D \sim \frac{\lambda_0^2}{\tau} \sim \frac{1/n^2}{1/n} \sim \frac{1}{n}$$

[n: particle density in gas]
[increases with pressure]



INCREASE the pressure!

Up to 4 atm possible

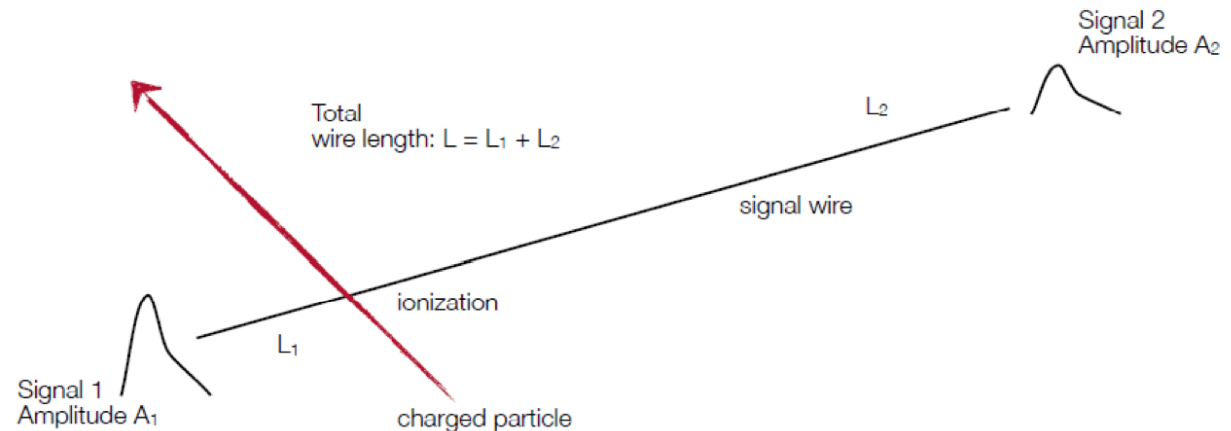
Position of coordinate along the wire

Possibilities to measure the position of the signal in the wire direction:

- **Charge division**: measure the current at both ends of anode wire:

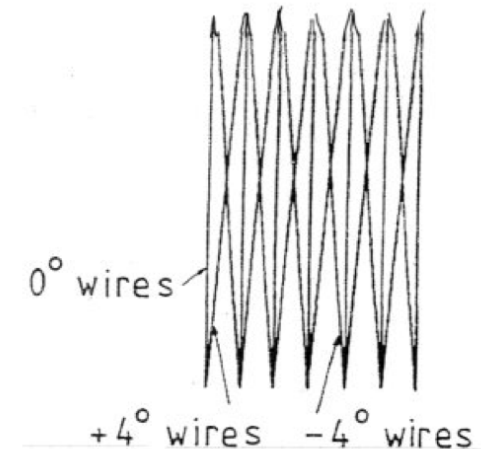
$$z \propto \frac{I_1 - I_2}{I_1 + I_2}$$

precision $\sim 1\%$ of wire length



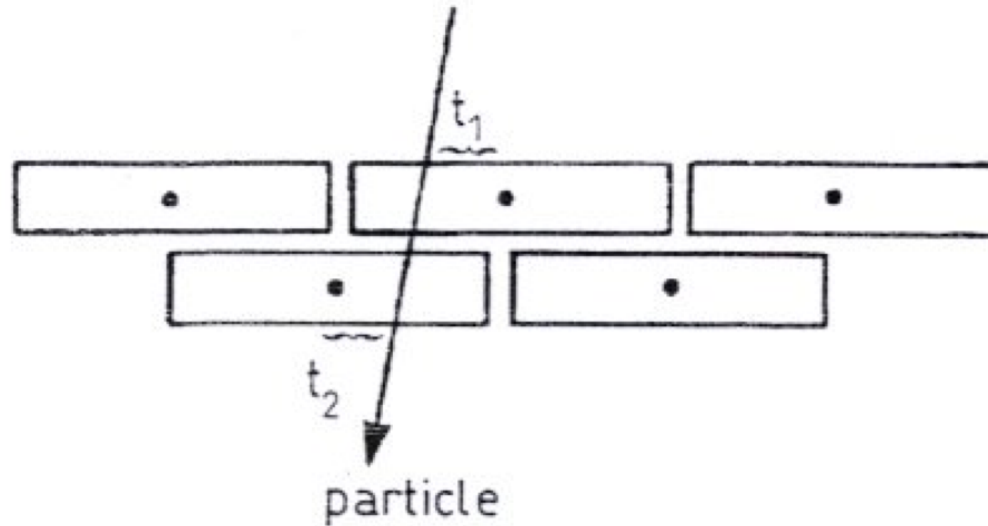
- **Time** measurement at both ends of the wire
- **Stereo wires**: layer of anode wires inclined by a small angle γ ("stereo angle") \rightarrow

$$\sigma_z = \frac{\sigma_x}{\sin \gamma}$$



Drift chambers: staggered wires

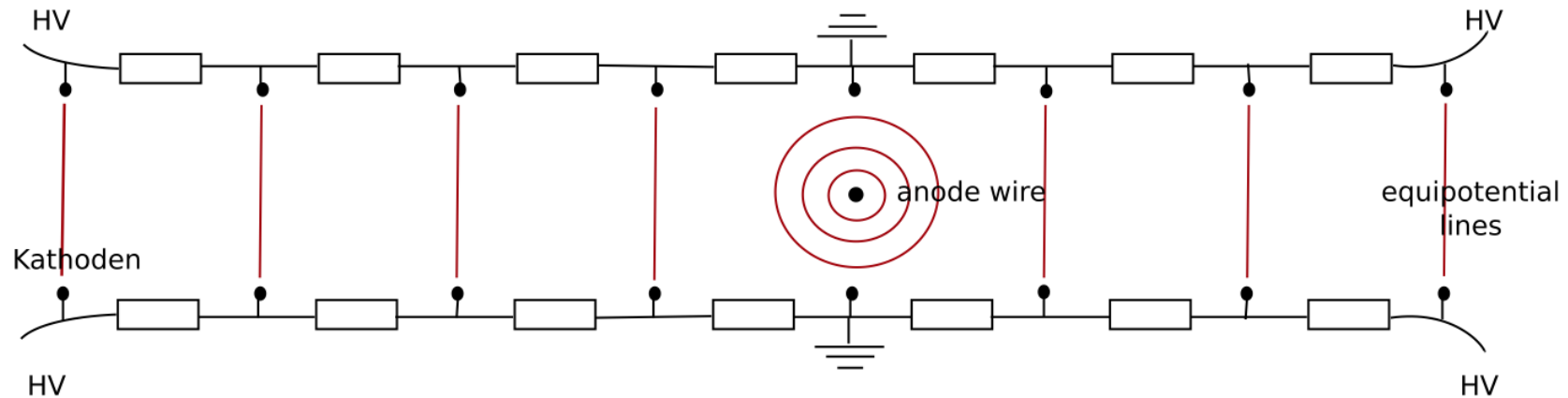
Difficulty: time measurement cannot distinguish between particle passing to the left or to the right of the anode wire → 'left – right ambiguity'



Use two layers displaced relative to each other by half the wire distance:
Staggered wires

Drift chambers: field and resolution

Very large drift chambers possible, introducing a voltage divider = cathode strips connected via resistors, and very few or even only one wire



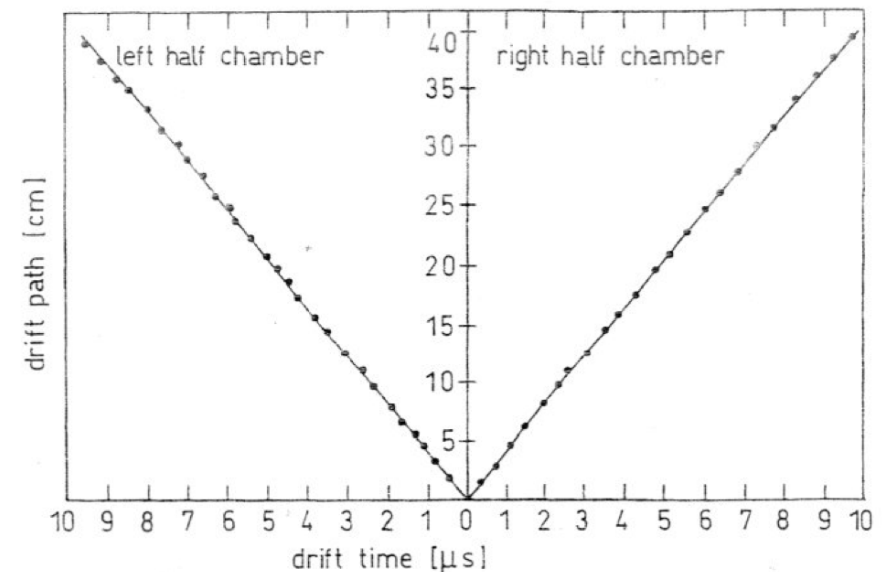
Space point resolution limited by mechanical tolerance:

Very large chambers:
100 cm x 100 cm → $\approx 200 \mu\text{m}$

Small chambers
10 cm x 10 cm → $\approx 20 \mu\text{m}$

Limit! The hit density has to be low!

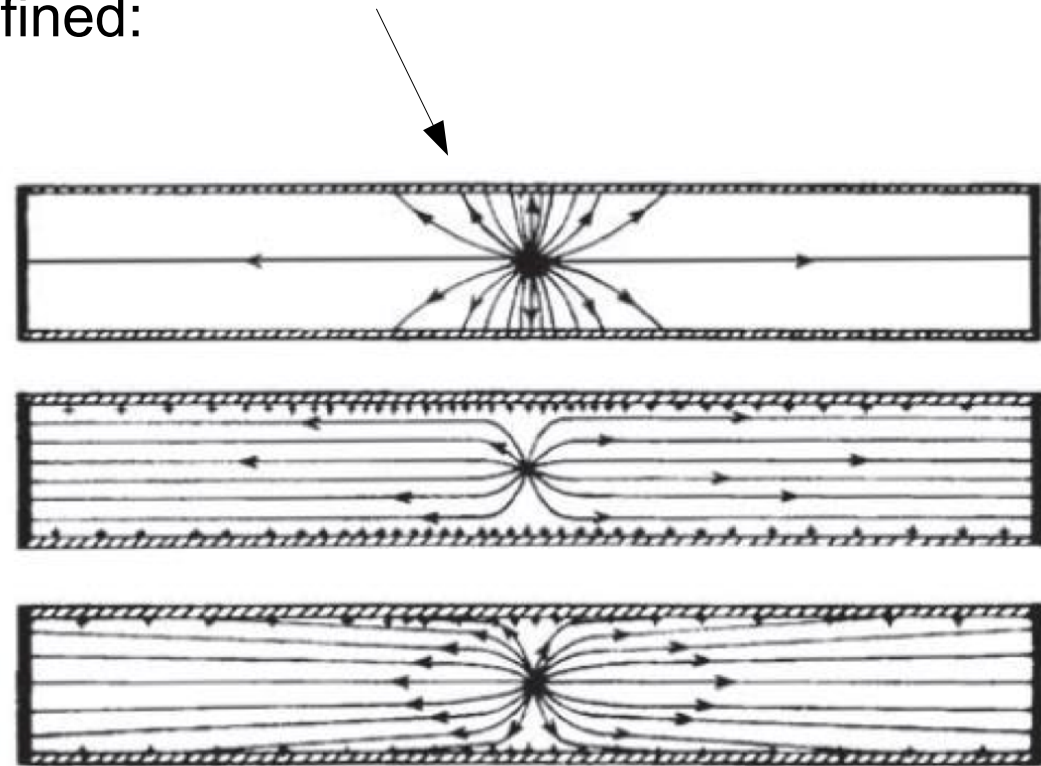
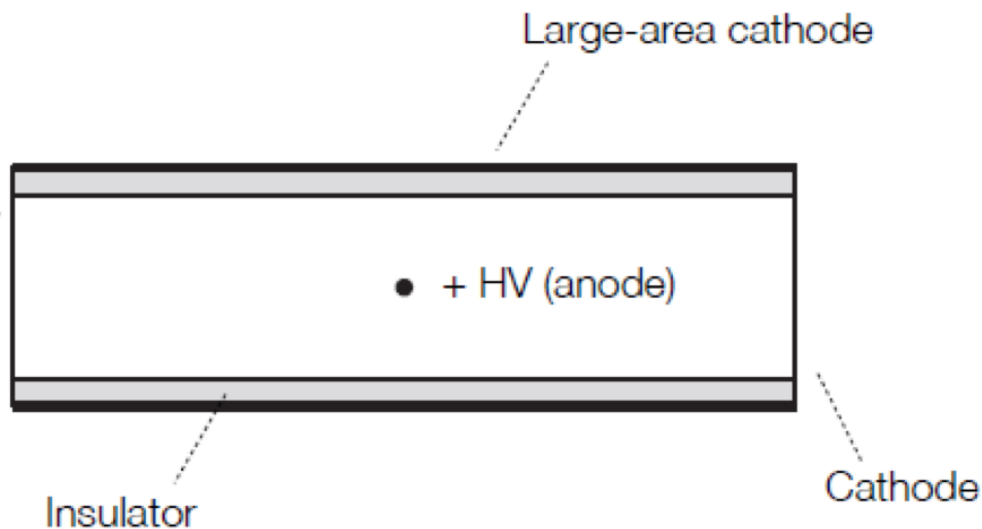
Drift time – space relation in a large drift chamber (80 cm x 80 cm) with only one anode wire (Ar + isobutane 93:7)



Resistive plate chambers

Electrode-less drift chamber:

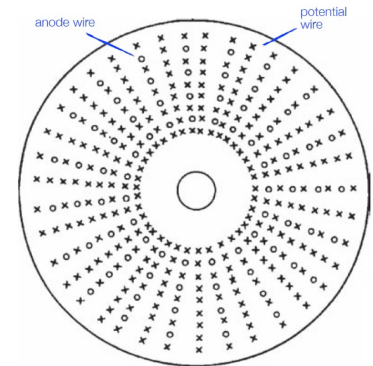
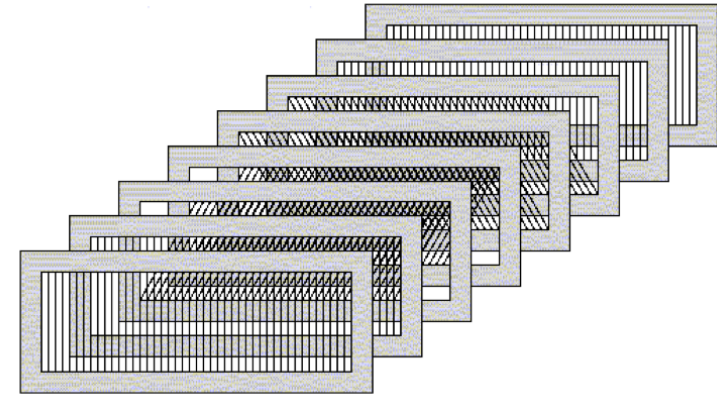
Field can be formed by charging up an insulating chamber wall with ions. After some charging time, ions cover the insulating layer → no field lines end there and the drift field is well defined:



To avoid overcharging, finite resistance of the insulator (some field lines end at the cathode)

Cylindrical wire chambers

- Fixed target experiments:
multi-layer MWPC or drift chambers
- Collider experiments, to cover the maximum solid angle:
 - Initially multi-gap spark chambers or MWPCs
 - Later cylindrical drift chambers, jet chambers
 - Today Time Projection Chambers (TPC)



Generally these chambers are operated in a magnetic field → measurement of radius ρ of curvature of a track
→ momentum determination (internally in one detector)

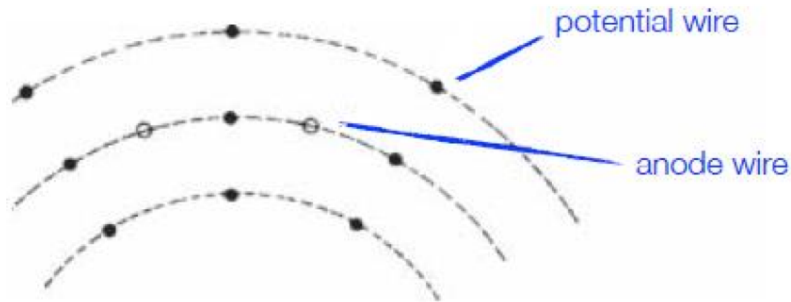
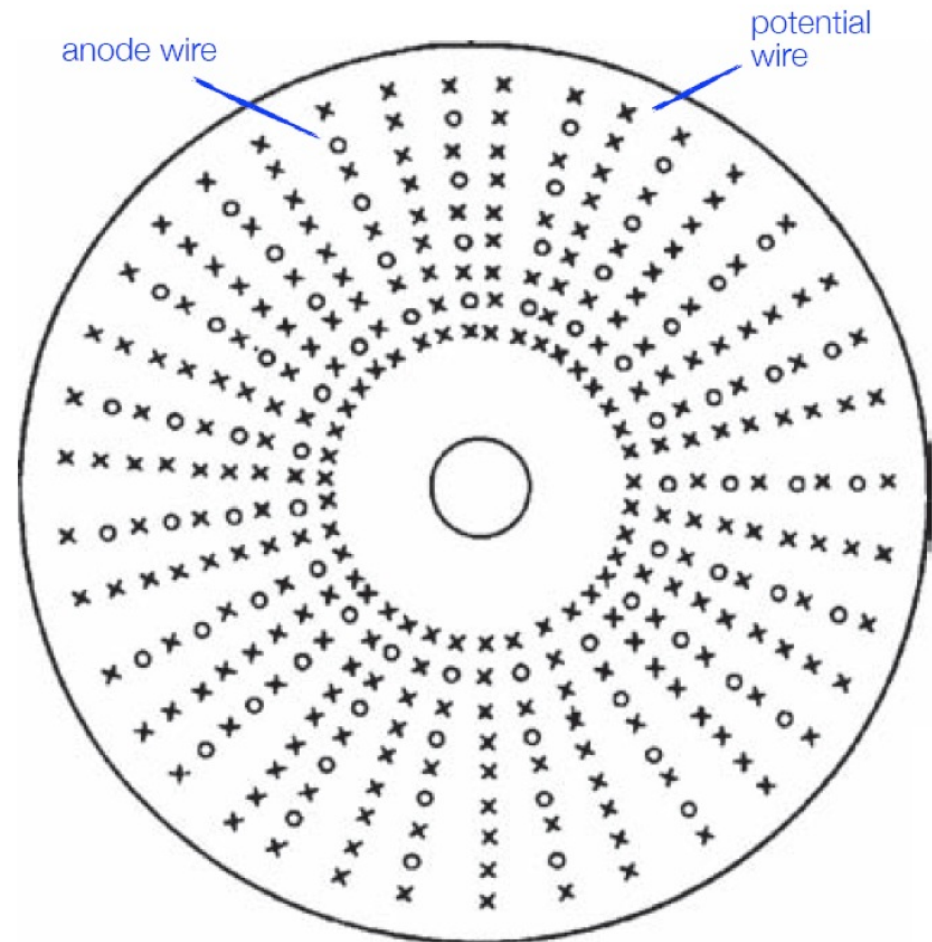
$$p \text{ (GeV/c)} = 0.3 \cdot B \text{ (T)} \cdot \rho \text{ (m)}$$

Cylindrical drift chambers

Principle of a cylindrical drift chamber: wires in axial direction, parallel to the beam axis AND the magnetic field

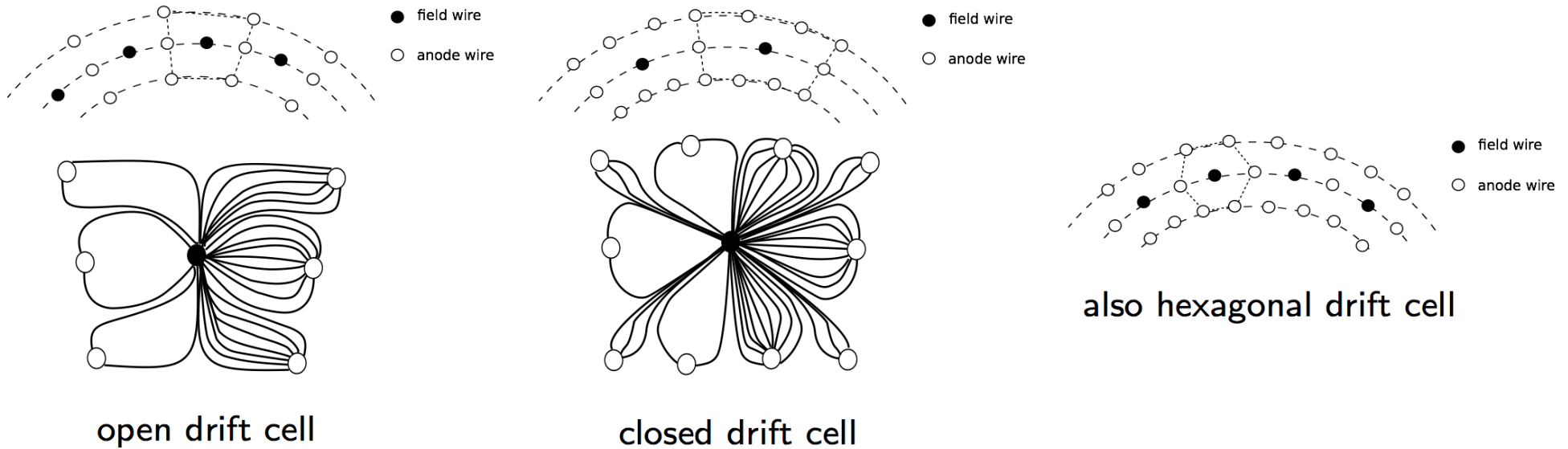
Alternating anode and field wires:

- One field wire between two anode wires
- Cylindrical layers of field wires between layers of anode wires → very good drift cell



Cylindrical drift chambers: cell geometries

Different drift cell geometries:



- Thin anode wires ($\varnothing \approx 30 \mu\text{m}$)
- Thicker field wires ($\varnothing \approx 100 \mu\text{m}$)
- Field quality better with more wires per drift cell

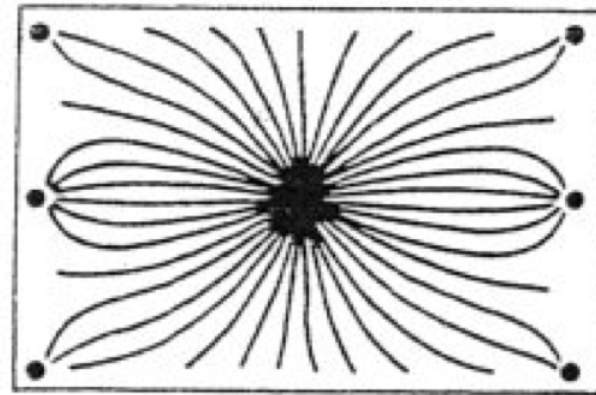
However:

- More labor-intensive construction
- Wire tension applies enormous stress on the end plates (e.g. 5000 anode wires + 15000 field wires \rightarrow 2.5 t on each end plate!)

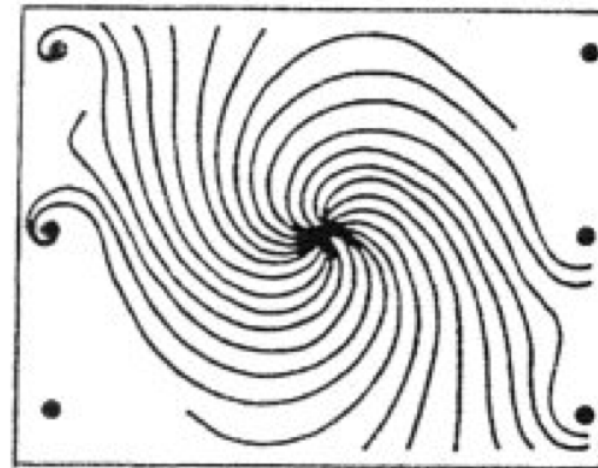
In $E + B$ fields

Here in general the electric drift field E is perpendicular to the magnetic field $B \rightarrow$ Lorentz angle for drifting charges must be considered!

Drift trajectories in an open rectangular drift cell for:
a) without, and
b) with magnetic field



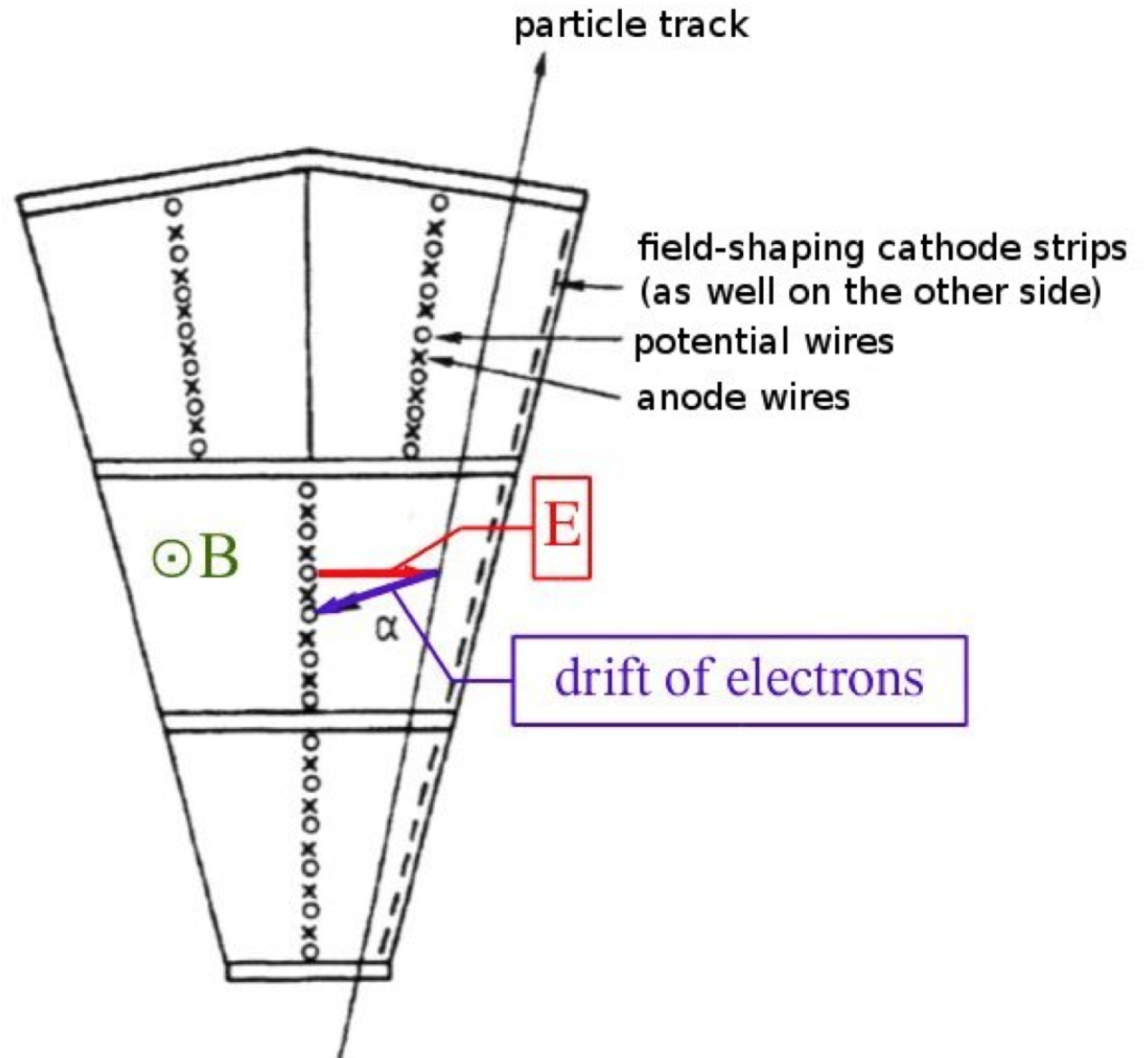
(a)



(b)

Jet drift chambers

- Very large drift cells
- Optimize number of measurements per track
Typically 1/cm

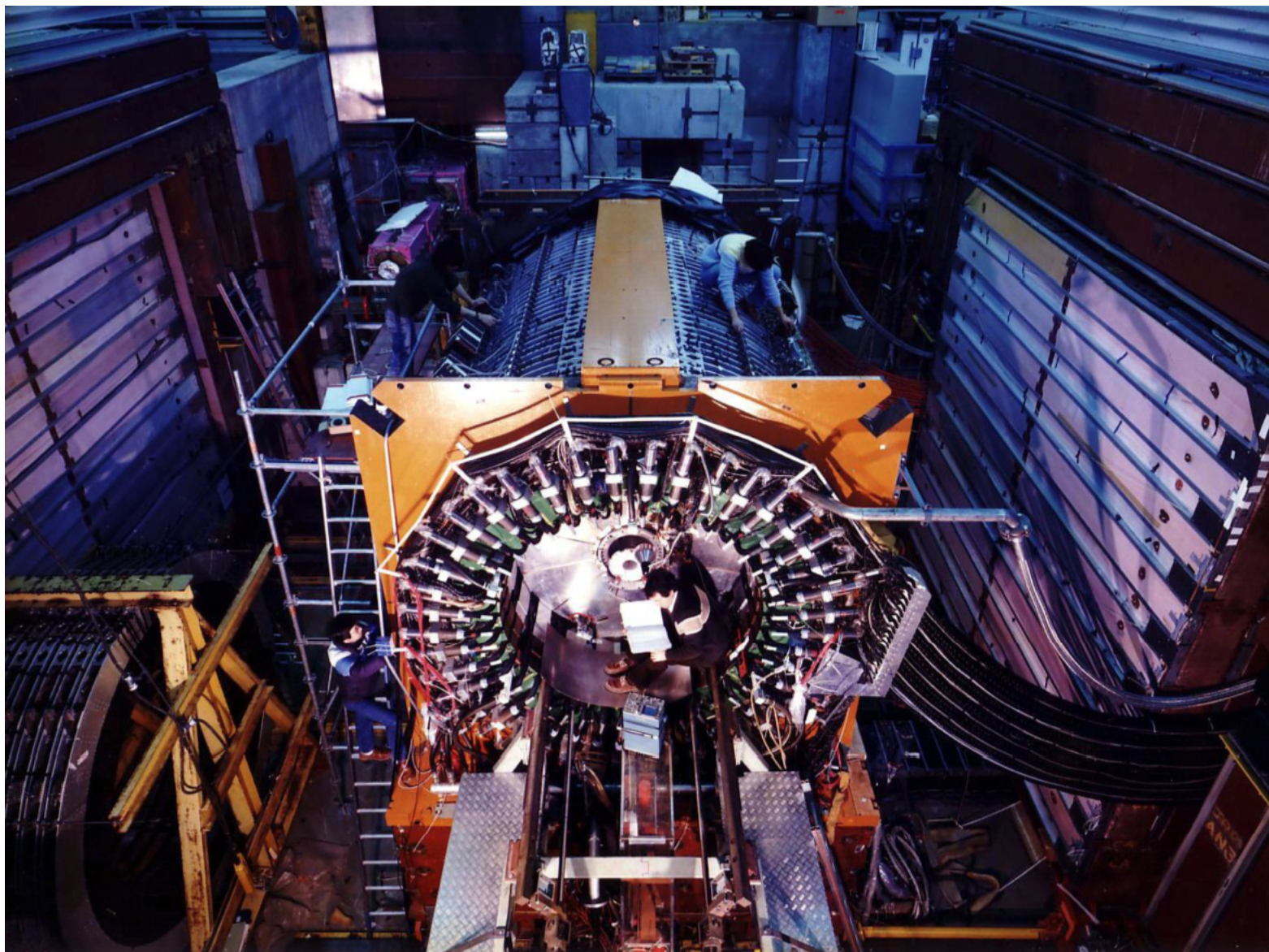


JADE jet chamber for PETRA (DESY)

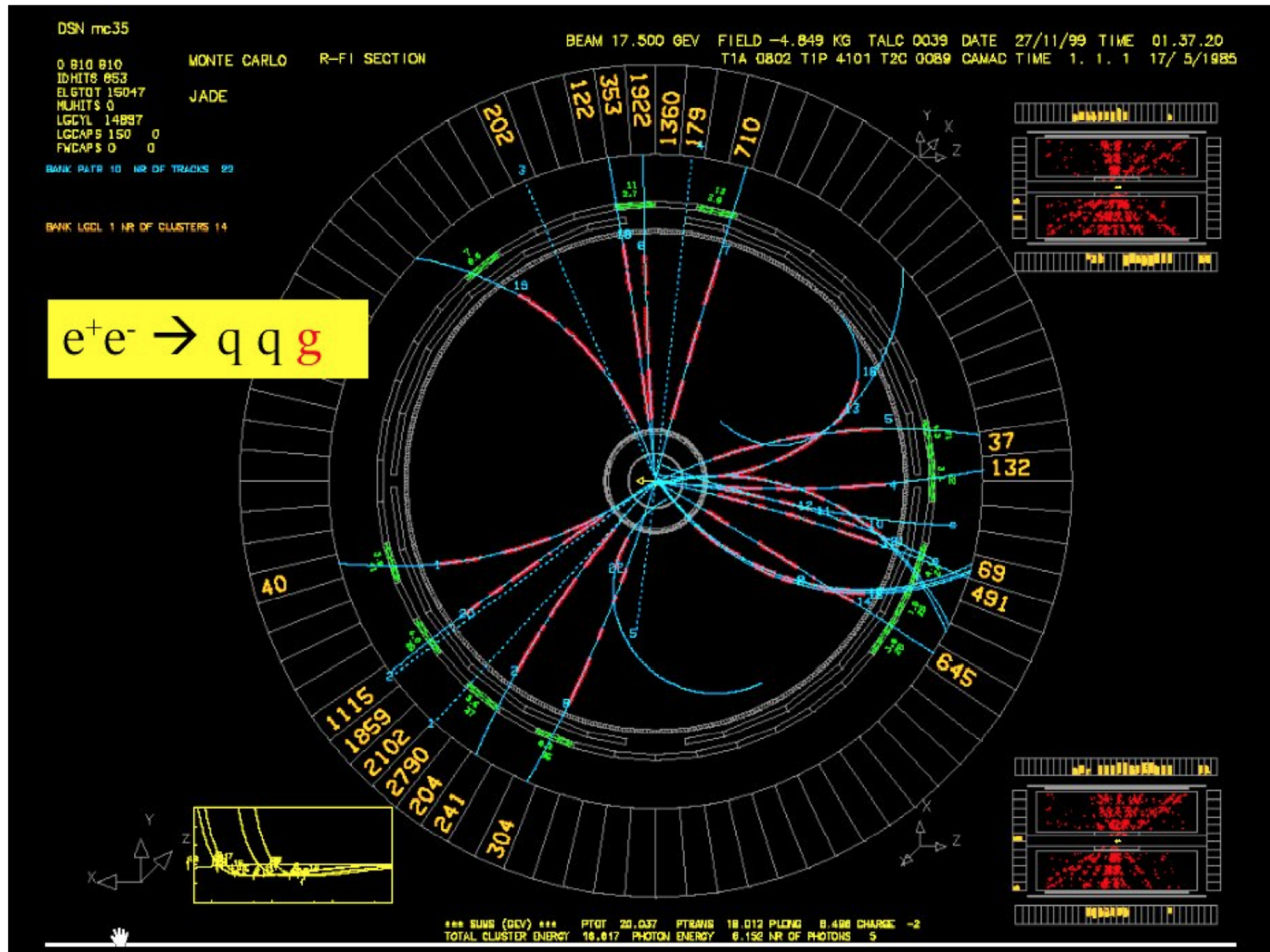
example: JADE jet chamber for PETRA, built by J.Heintze et al. Phys. Inst. U. Heidelberg
length: 2.34 m, radial track length: 57 cm, 47 measurements per track
 $\sigma_{r\phi} = 180 \mu\text{m}$, $\sigma_z = 16 \text{ mm}$



JADE jet chamber for PETRA (DESY)



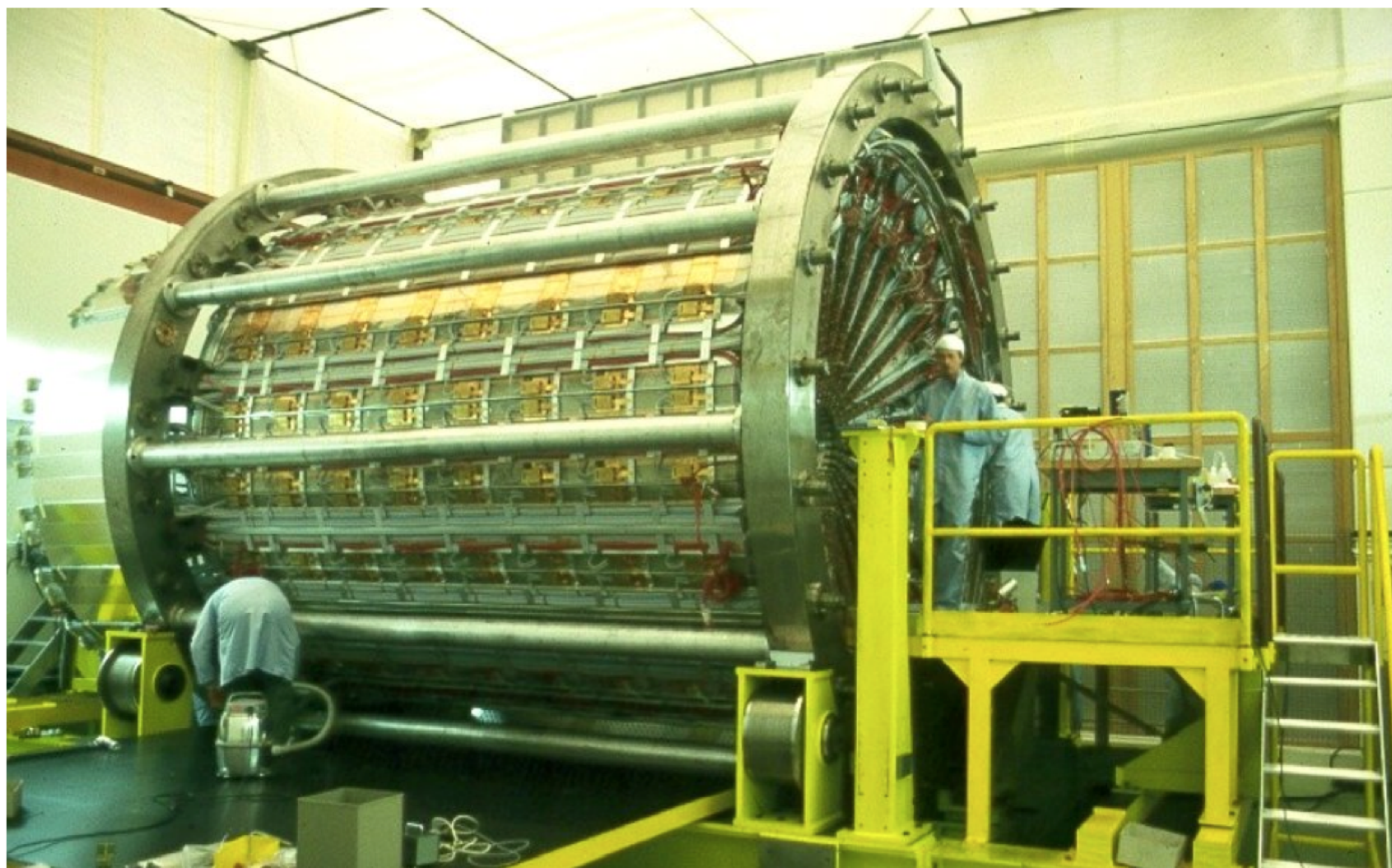
JADE jet chamber for PETRA (DESY)



3-jet event by JADE – measurements taken at PETRA → discovery of gluon

Jet chamber in OPAL, at LEP

length: 4 m, radius: 1.85 m, 159 measurements per track, gas: Ar/CH₄/C₄H₁₀ at 4 bar
 $\sigma_{r\phi} = 135 \mu\text{m}$, $\sigma_z = 60 \text{ mm}$



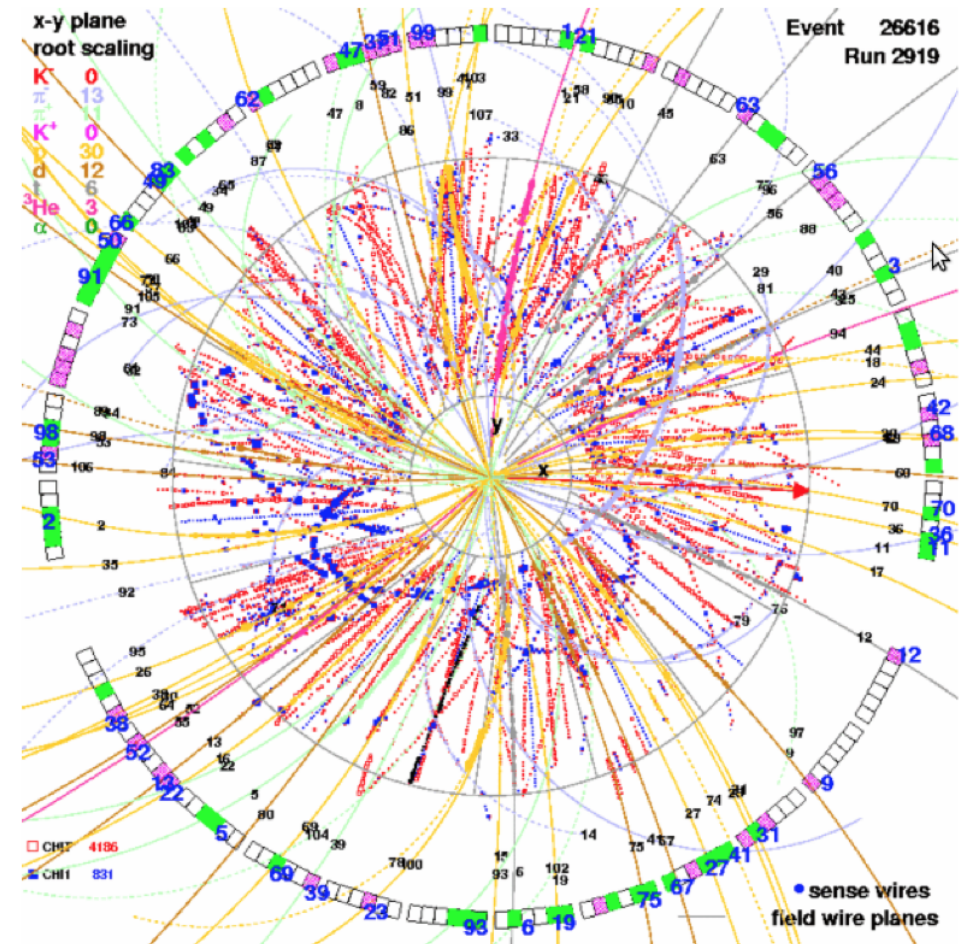
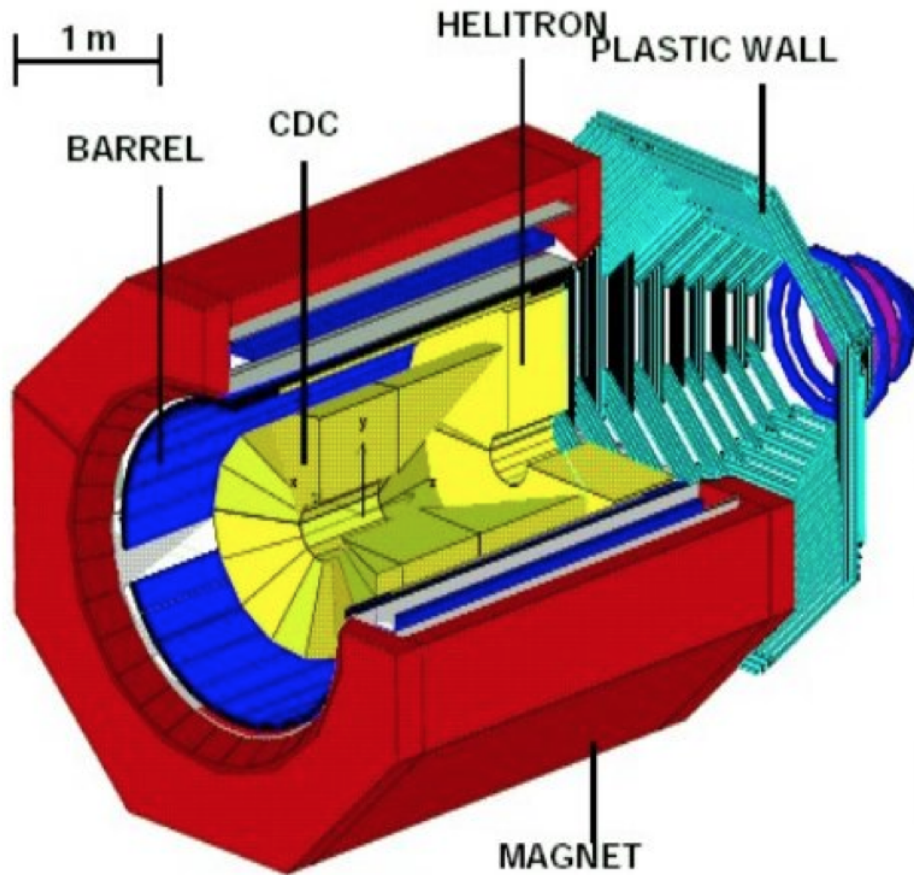
Jet chamber in OPAL, at LEP

interior of jet chamber of OPAL



Central drift chamber (CDC) in FOPI

application for heavy ion collisions: FOPI (experiment at SIS at GSI):
central drift chamber (CDC), D. Pelte and N. Herrmann Phys. Inst. U.Heidelberg



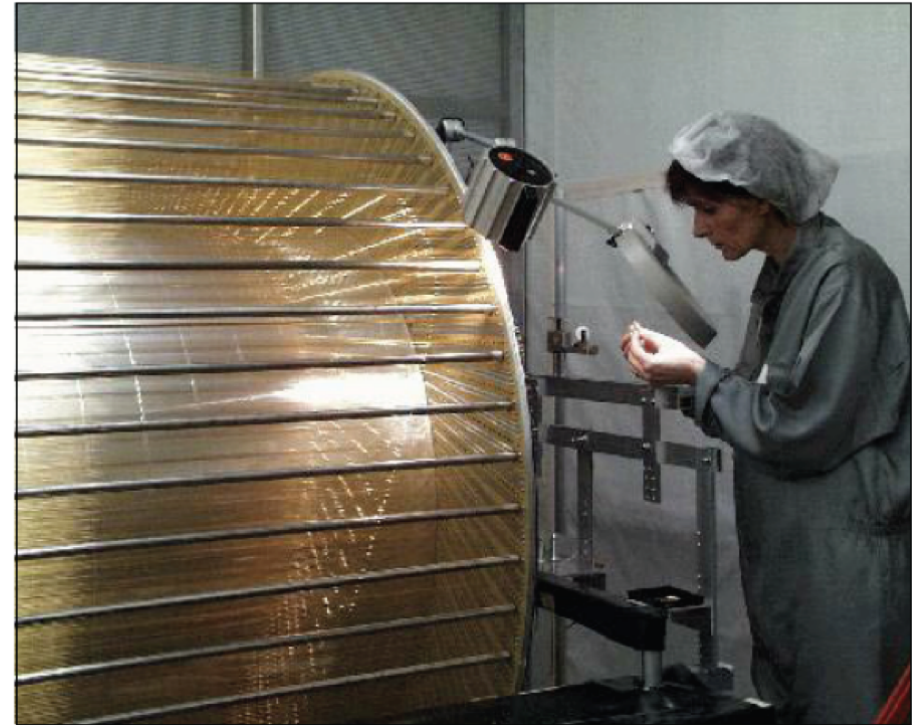
H1 cylindrical drift chamber



Cylindrical
Drift Chamber

[H1 Experiment]

Number of wires: ~ 15000
Total force from wire tension: ~ 6 t

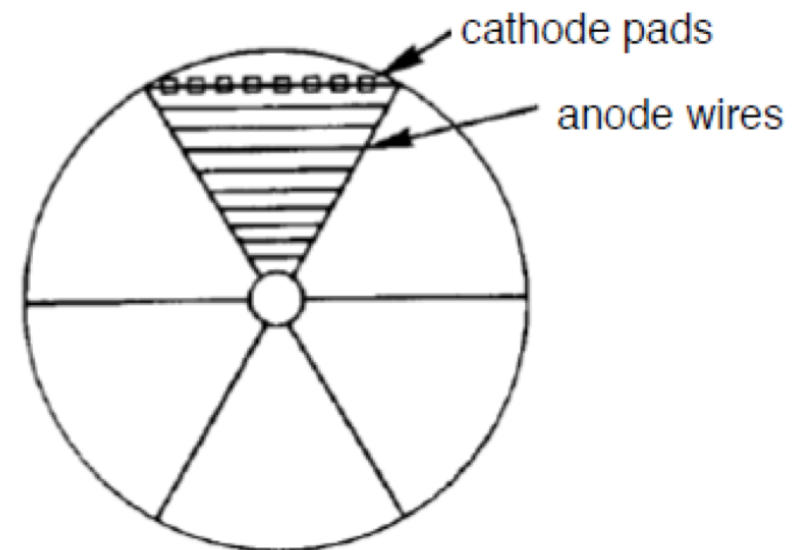
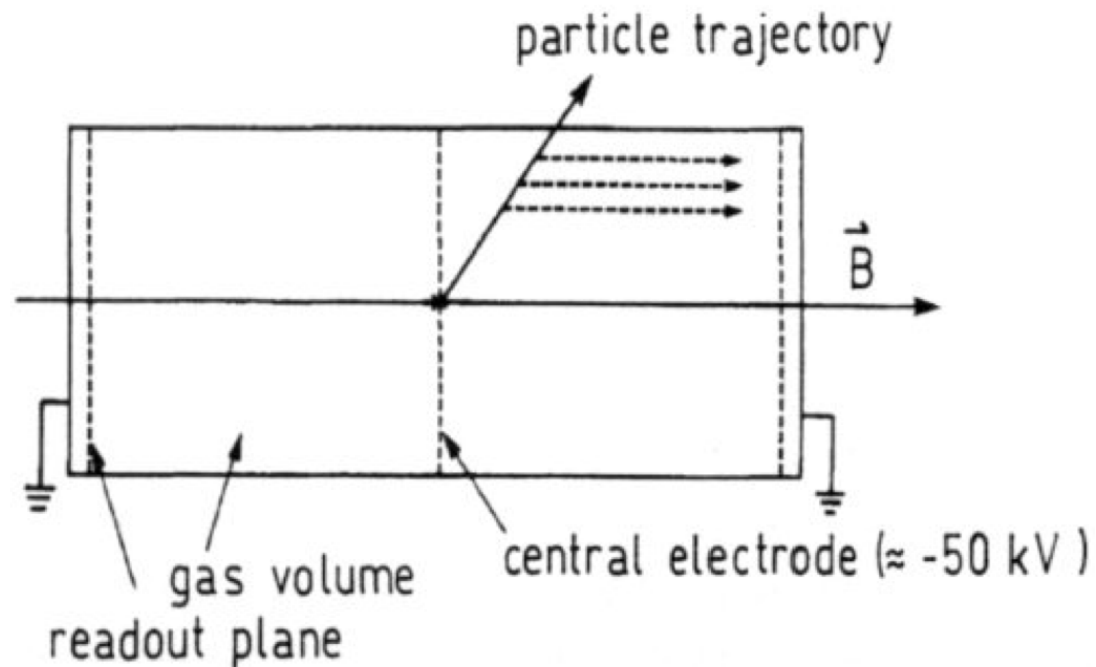


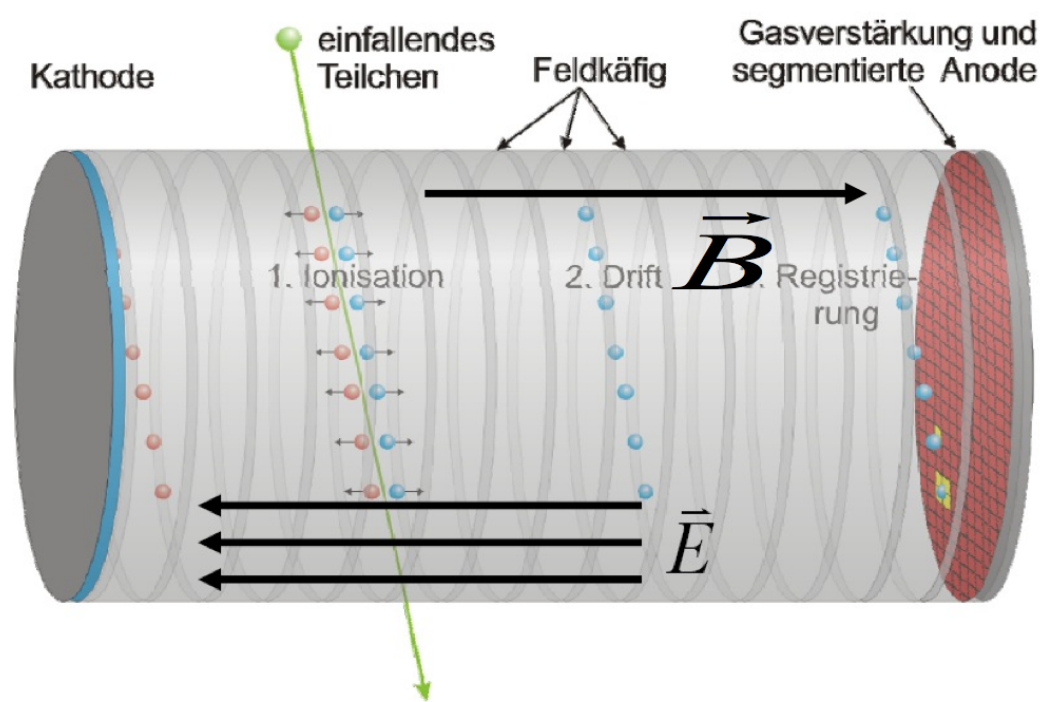
Time Projection Chamber

“Electronic bubble chamber”
Full 3D track reconstruction
Invented by D. Nygren (1974)
at Berkeley National Lab

- Mostly cylindrical detectors
- Central HV electrode
- MWPCs at the end-caps
- Usually $E \parallel B \rightarrow$ Lorentz angle = 0

- Particles traversing the gas produce charges by ionization
- Electrons drift towards the MWPC in a highly uniform E field
- Position (2D), arrival time, and energy deposited is measured





ADVANTAGES:

- Complete track determination within one detector → good momentum determination
- Relatively few wires
- Particle identification via dE/dx thanks to the charge measurement
- Drift parallel to B field → transversal diffusion suppressed by factors 10-100 → good spatial resolution

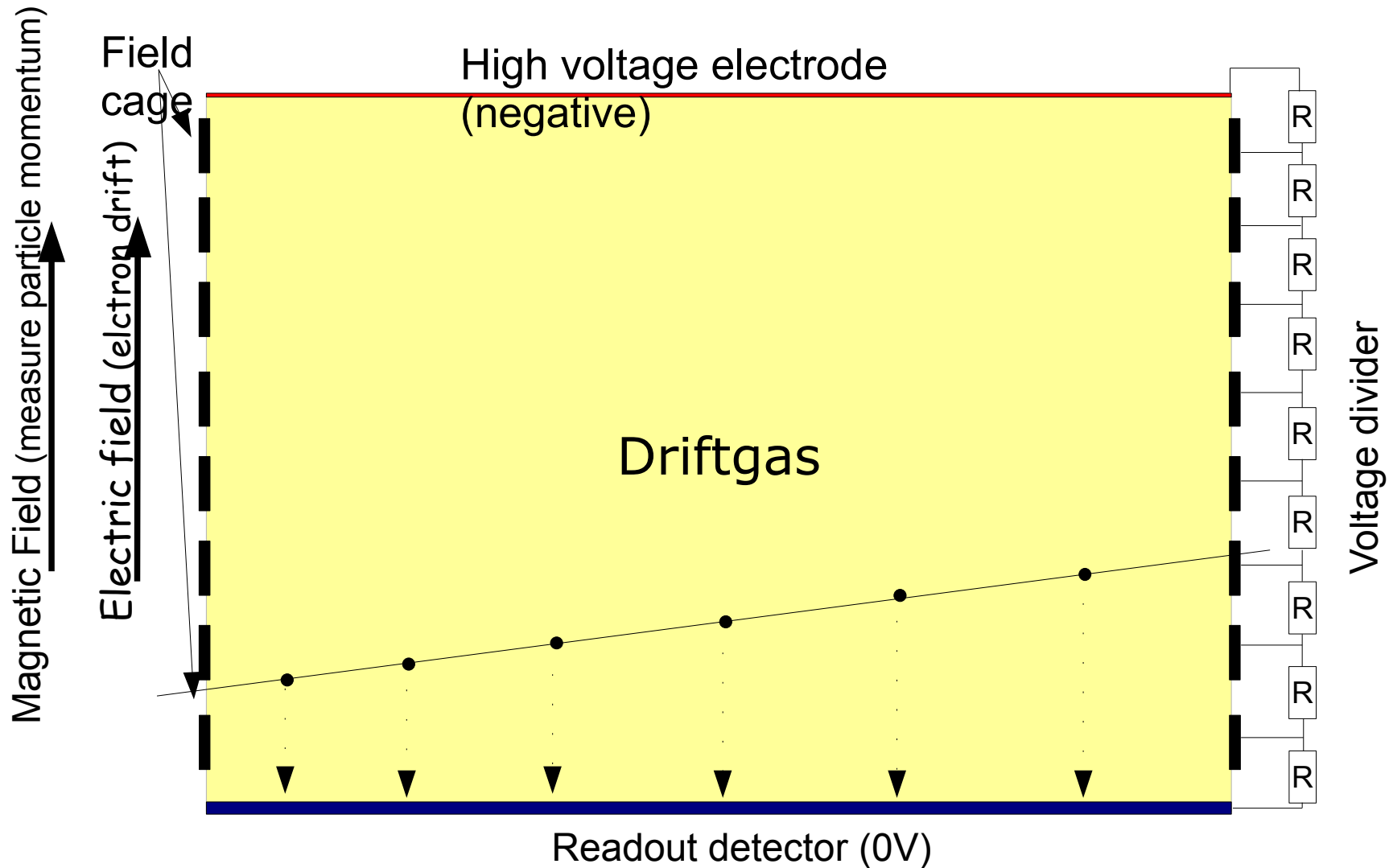
DISADVANTAGES, CHALLENGES

- Drift time relatively long, 10-100 μs → not a high rate detector. Attachment
- Large volume (precision)
- Large voltage (discharges)
- Large data volume

Structure of a TPC

Highly uniform electric field obtained with field cage

Watch! We rotate by 90° wrt previous sketches



TPC: principle of operation

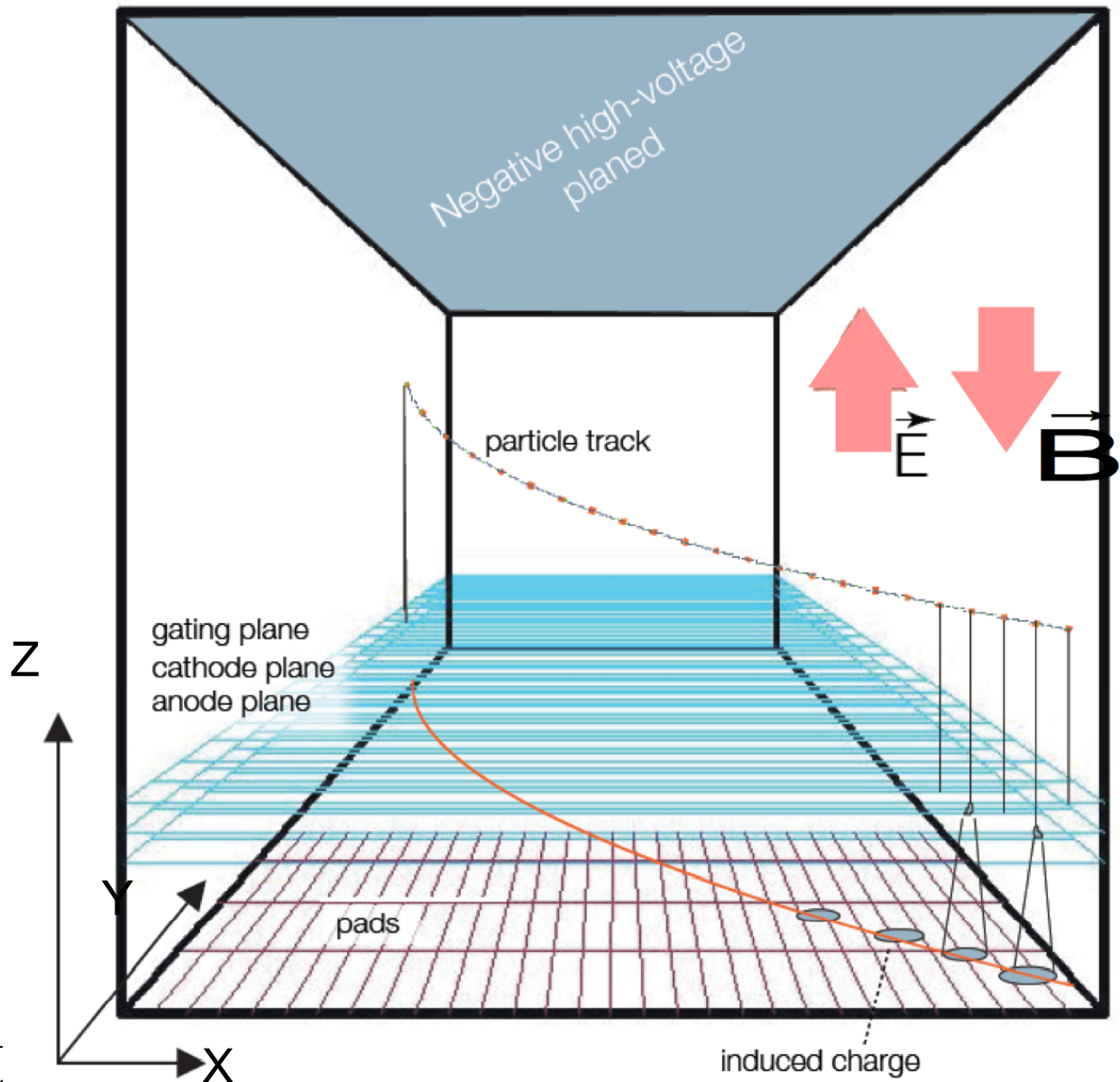
Ionization electrons move towards the MWPC along the E field lines.

At the end of the long drift path, the signal is induced on the anode wires and the cathode pads. They are continuously sampled.

- Z-coordinate is given by the drift time (v_{drift} critical!)
- X-coordinate is given by charge sharing among cathode pads
- Y-coordinate is given by the wire and pad row number

True 3-dimensional measurement of the ionization points of the entire tracks.

High multiplicity of tracks possible!



TPC: principle of operation

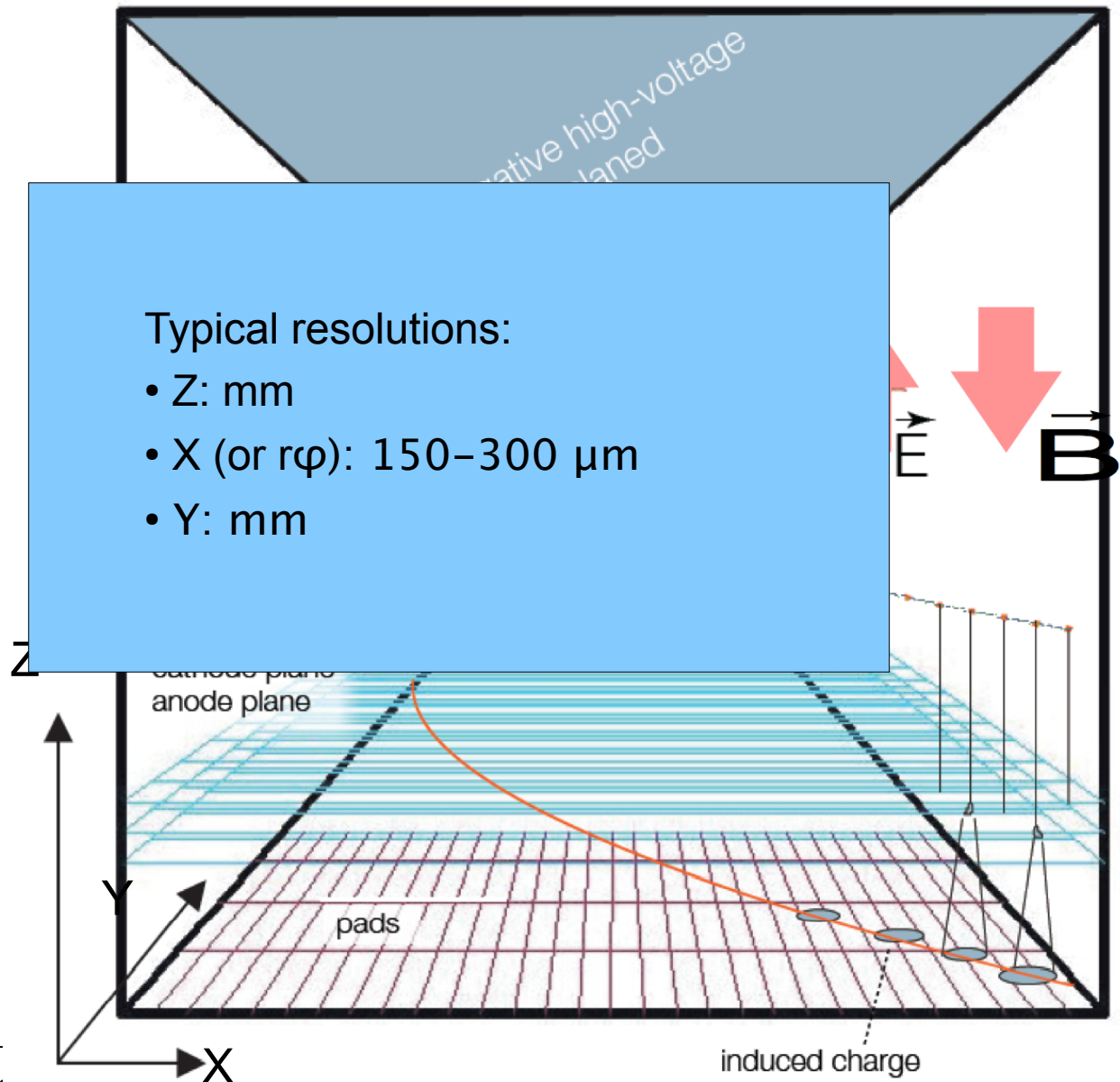
Ionization electrons move towards the MWPC along the E field lines.

At the end of the long drift path, the signal is induced on the anode wires and the cathode pads. They are continuously sampled.

- Z-coordinate is given by the drift time (v_{drift} critical!)
- X-coordinate is given by charge sharing among cathode pads
- Y-coordinate is given by the wire and pad row number

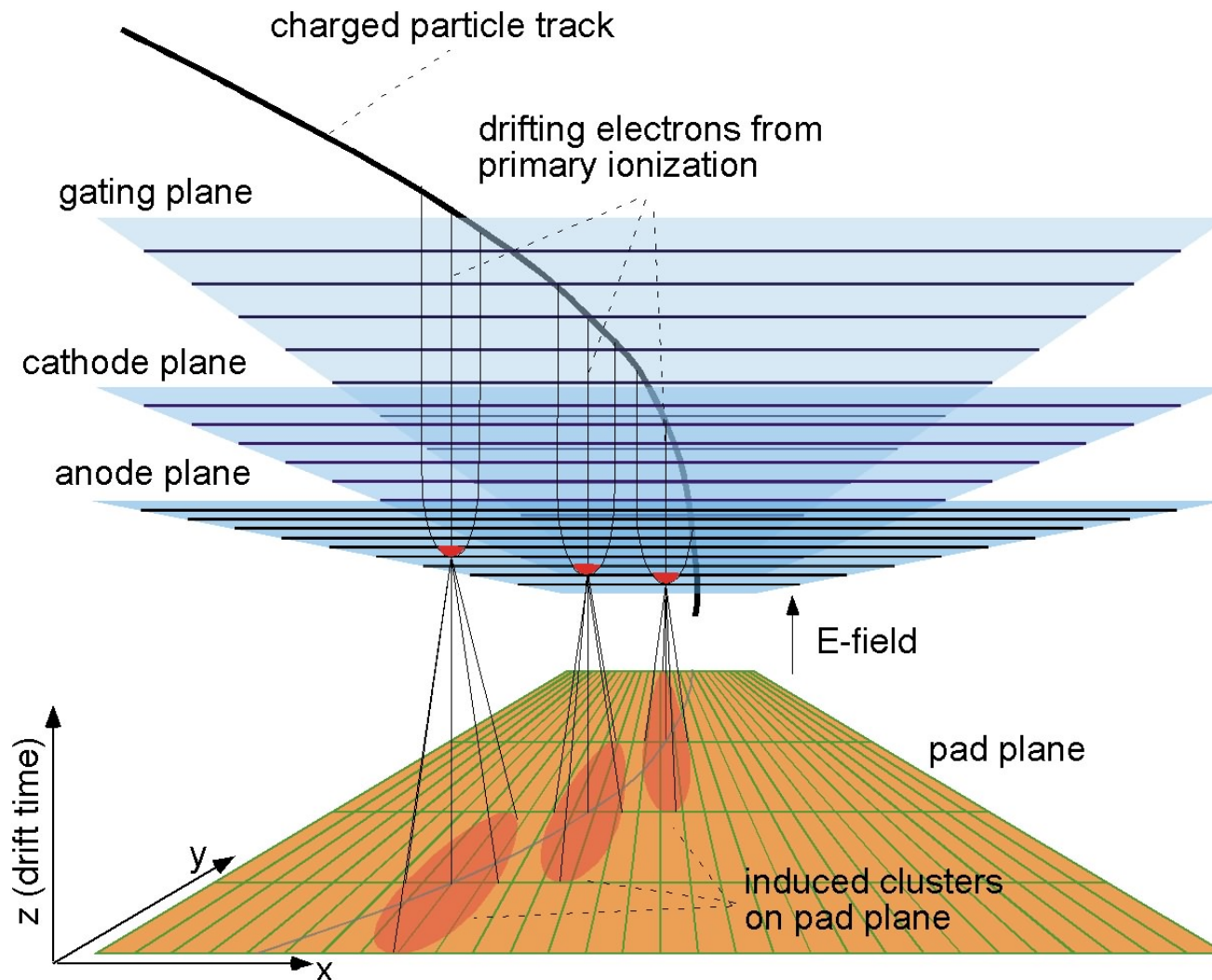
True 3-dimensional measurement of the ionization points of the entire tracks.

High multiplicity of tracks possible!



TPC: wire chambers

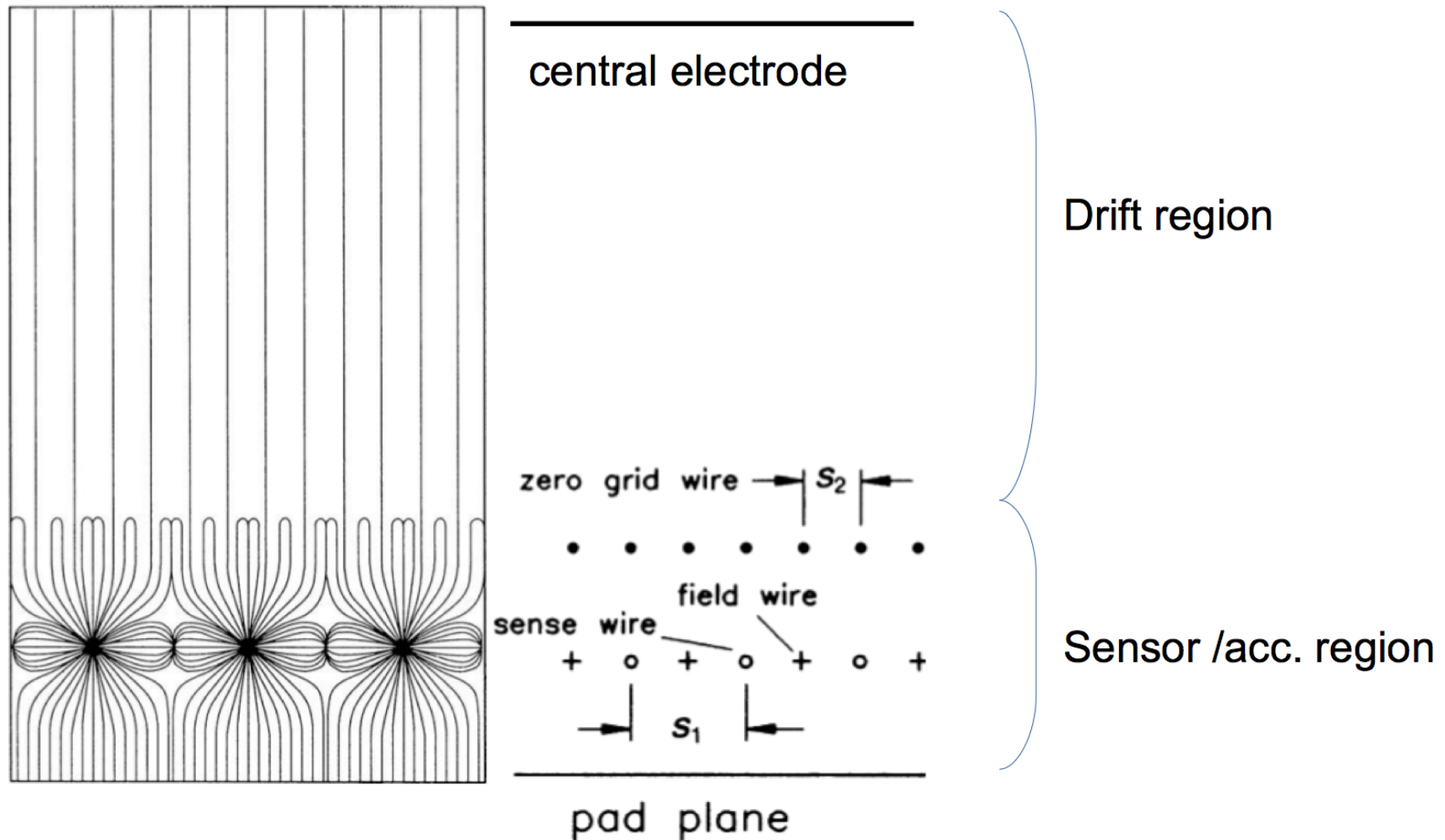
Several wire planes for optimal field shaping and to stop ion back-flow (see next slide)



TPC: wire planes

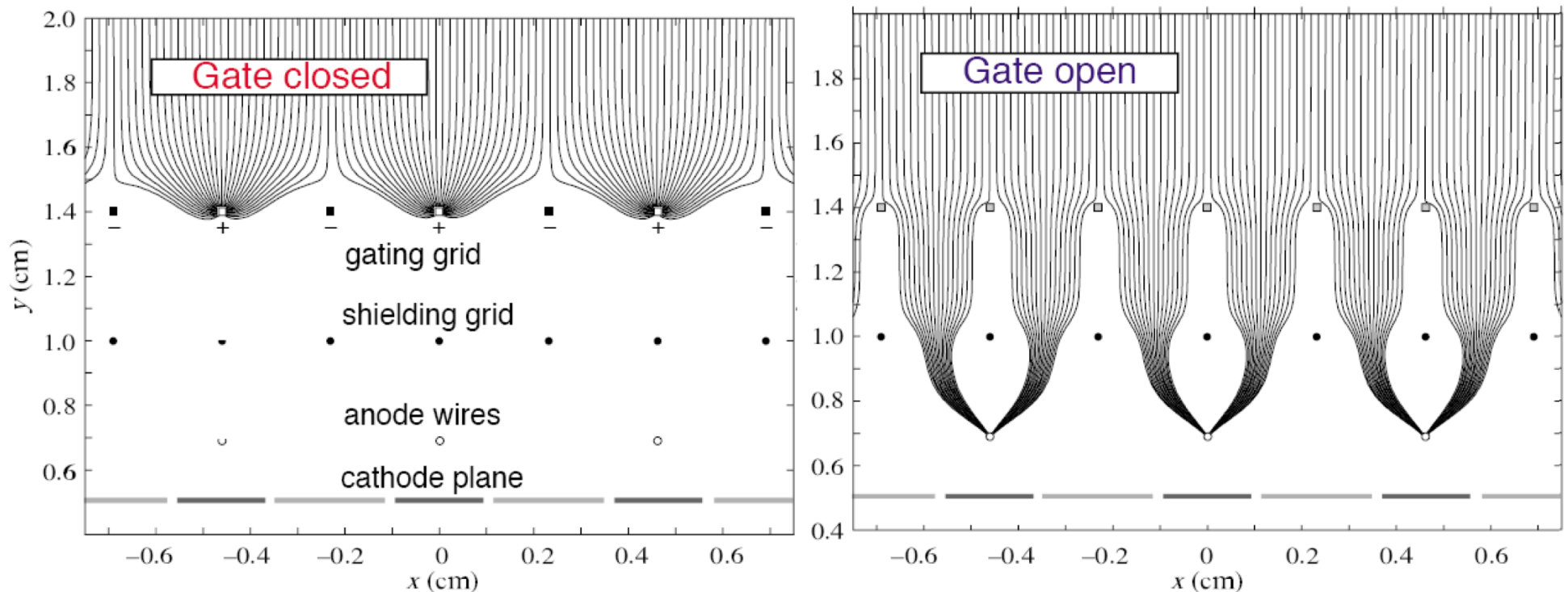
Double layer of wires to shape E-field lines in the region of anode wires

E-Field of a wire grid



TPC: ion back flow \leftrightarrow gating grid

- After the charge multiplication around the anode wires, if the many ions move back to the drift region they would build a substantial space charge. This would cause serious distortions of the drift field!
- Use a **gating grid** which collect the ions and stop them from moving back into the drift region
- The shielding wire layer in between protect the sense wire from possible disturbance while switching



TPC: gating grid

- An external trigger switches the gating grid. It is by default kept closed: upon an interaction trigger, the grid is opened
- It remains opened for the maximal time of drift of electrons from the active volume, then closes again to keep the ions from the amplification away from the drift region

Limitation:

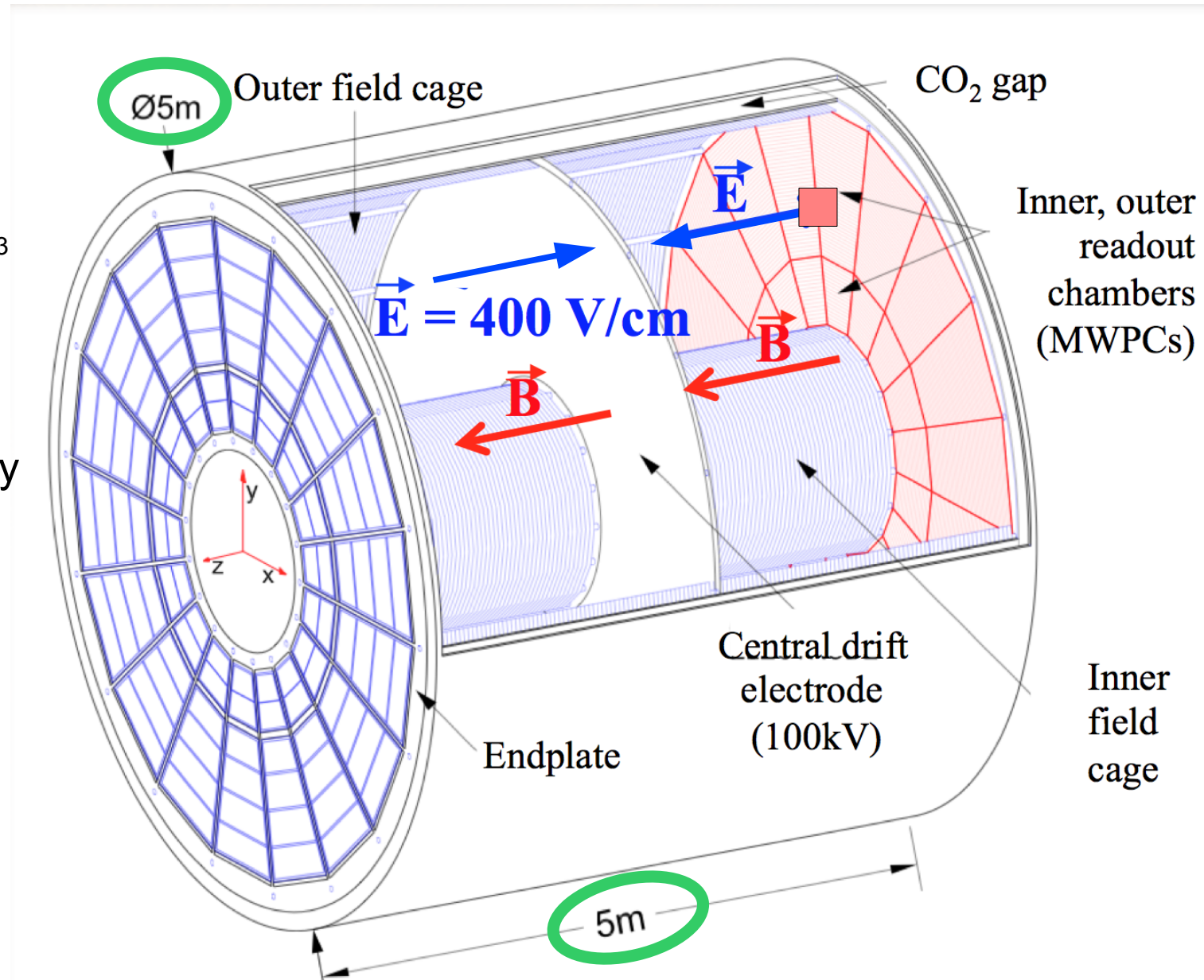
The relatively long drift times ($\sim 100 \mu\text{s}$ for electrons!) and the operation with gating grid limits the effective live time of the detector, and its maximal readout rate!!

→ ALICE TPC upgrade: from MWPC + gating grid → GEM chambers

ALICE TPC

LARGEST TPC EVER BUILT

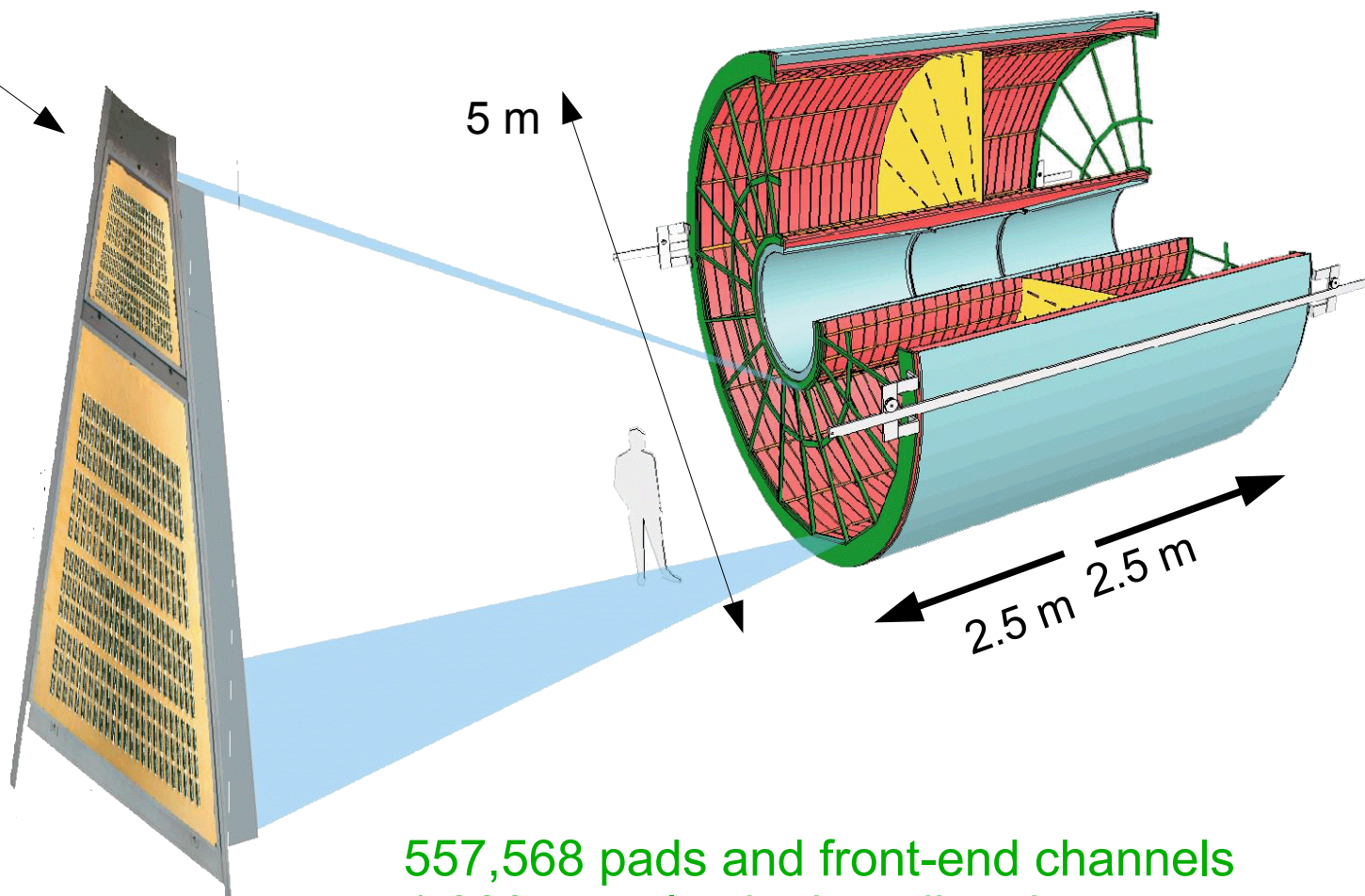
- Gas volume: $\sim 92 \text{ m}^3$ (active volume)
- Very light giant: 3% X_0 at mid-rapidity
- 72 readout chambers: Multi Wire Proportional Chambers with pad readout
- Half a million pads! (557,568 channels)



ALICE TPC: the readout chambers

- 2 end-plates with readout chambers, each with 18 sectors
- Each sector:

- Inner ReadOut Chamber (IROC)
- Outer ReadOut Chamber (OROC)

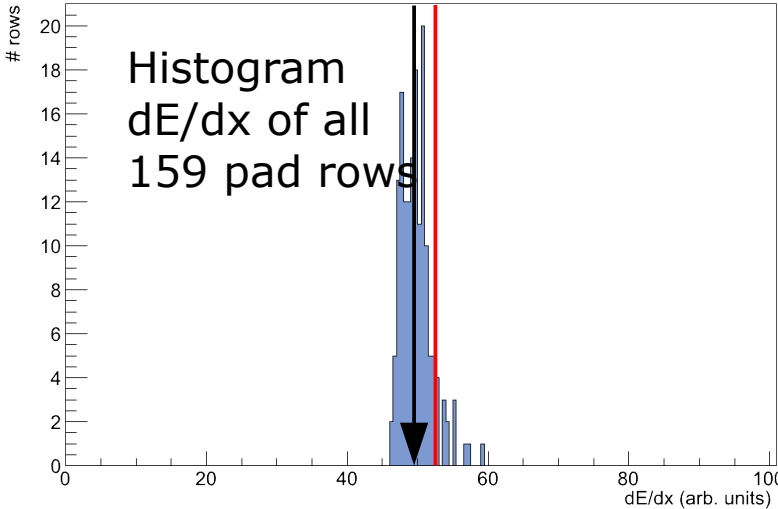
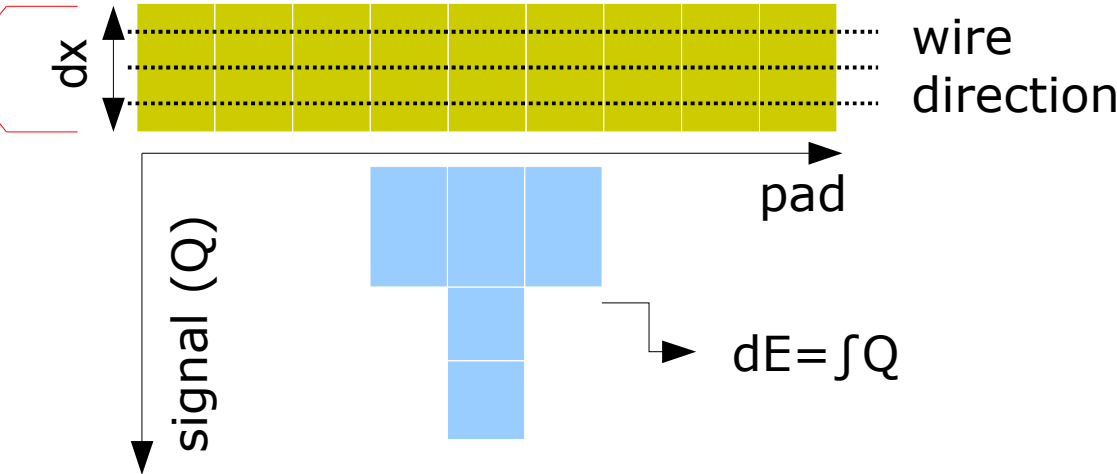
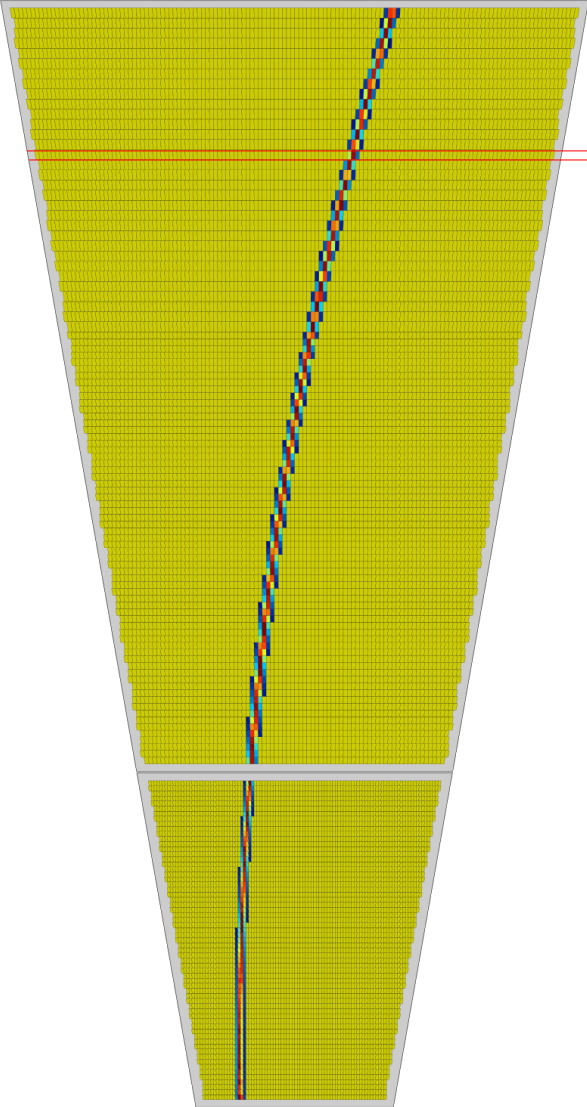


Drift voltage (central electrode): 100 kV
Anode voltage: 1350/1570 V
Nominal gain: 5000 - 8000

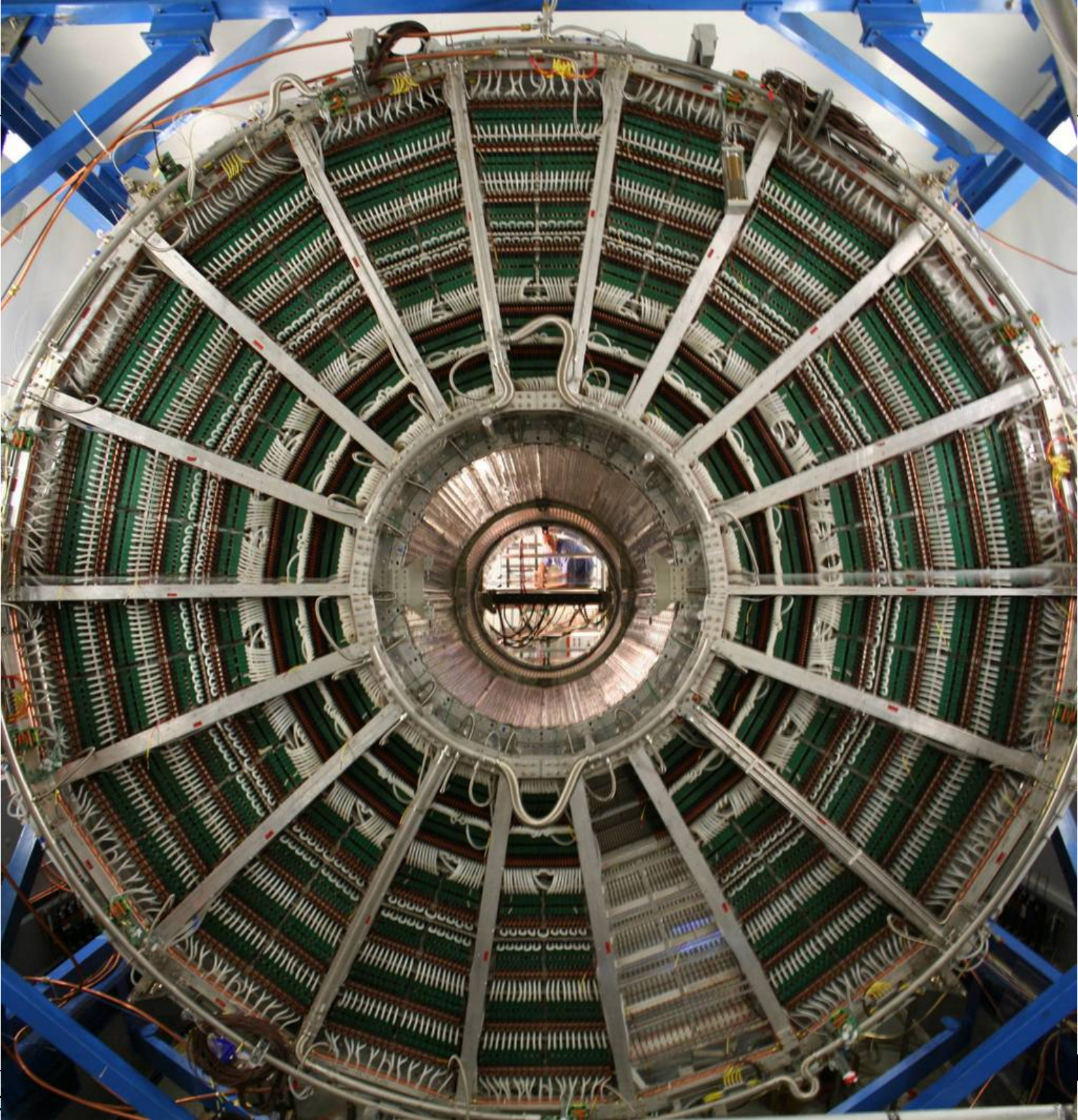
557,568 pads and front-end channels
1,000 samples in time direction
557 million voxels

ALICE TPC: dE/dx measurement for PID

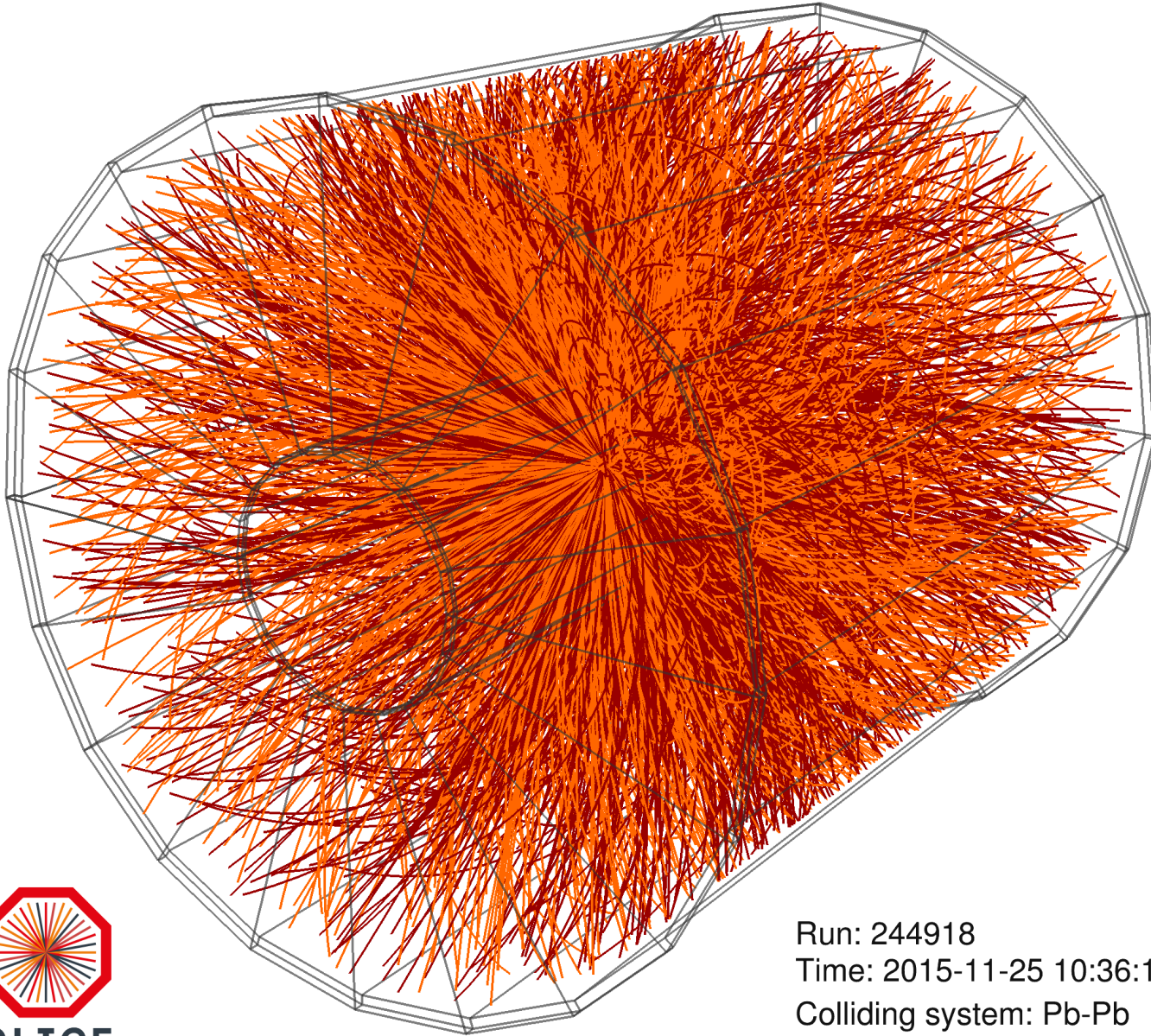
Resolution: ~ 5%



Truncated mean
($\langle dE/dx \rangle$) cutting
upper 40% of the
charge distribution
used as PID signal



ALICE TPC: event display



Run: 244918
Time: 2015-11-25 10:36:18
Colliding system: Pb-Pb
Collision energy: 5.02 TeV